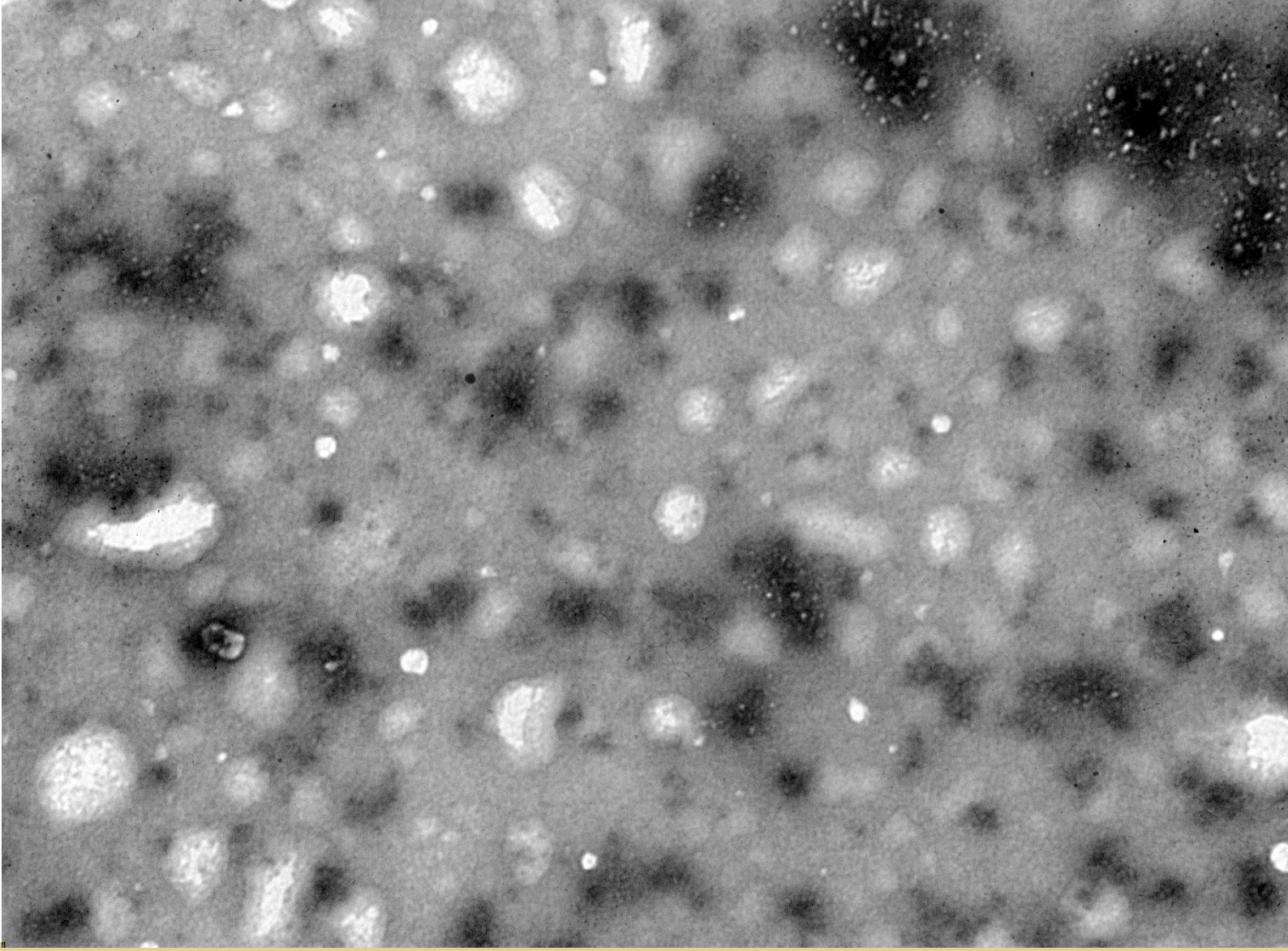

Vanessa Patrícia Dias Pinto

Comparison of Extracellular Vesicles isolation protocols from the plasma of patients with multiple myeloma: size characterization, expression of EV markers and microRNAs

Master Dissertation in Cellular and Molecular Biology

Coimbra

September 2016

· U C ·

UNIVERSIDADE DE COIMBRA

Vanessa Patrícia Dias Pinto

Comparison of Extracellular Vesicles isolation protocols from the plasma of patients with multiple myeloma: size characterization, expression of EV markers and microRNAs

Dissertation presented to obtain the Master's Degree in Cellular and Molecular Biology at Faculty of Sciences and Technology of the University of Coimbra, Portugal

Work performed under the supervision of Prof. Doutora M. Helena Vasconcelos (Department of Biological Sciences, Faculty of Pharmacy of the University of Porto) and co-supervision of Prof. Doutora Emília Duarte (Department of Life Sciences of the University of Coimbra)

UNIVERSIDADE DE COIMBRA

Experimental activities described in this thesis were performed at the Cancer Drug Resistance group from the IPATIMUP/i3S institute (Institute of Molecular Pathology and Immunology/Institute for Innovation and Health Research) of the University of Porto (Porto, Portugal). The present work was developed under supervision of Prof. Doutora Helena Vasconcelos (Department of Biological Sciences, Faculty of Pharmacy of the University of Porto) and tutorial support of Doutor Hugo Seca Teixeira (Faculty of Sciences of the University of Porto).

Instituto de Patologia e Imunologia Molecular da Universidade do Porto

Agradecimentos

À Professora Doutora M. Helena Vasconcelos agradeço por todo o seu apoio, pela atenção dispensada, paciência e conhecimento transmitido. Um muito obrigada.

Ao grupo "Cancer Drug Resistance", ao Hugo Seca e Rui Bergantim pelo apoio ao longo do projecto. À Diana e à Vanessa por se mostrarem disponíveis a ajudar-me. E um especial agradecimento à Cristina Xavier por tudo o que me ensinou e à Inês Silva pelo companheirismo e a ambas pela amizade verdadeira.

Às colegas de laboratório Ana João e Flávia Castro pela boa disposição e pela amizade.

Aos meus amigos da faculdade, em especial à Fernanda e à Silvie que me apoiaram em tempos menos fáceis e me acompanharam noutros quantos especiais, pelo companheirismo e pela ajuda.

À família que eu escolhi, aos melhores amigos que podia ter, pela compreensão perante as minha ausências e por continuarem sempre ao meu lado, à Ana, à Sílvia, à Pipa, ao Jomi, ao Ivo, ao Diogo, ao Rato, à Raquel, à Janete e ao Rodrigo. Pela amizade mais verdadeira e pela força. Pelos sorrisos.

À minha família, por tudo o que me ensinaram, pela educação que me deram, por me fazerem crescer e sentir apoiada. Um especial agradecimento aos meus avós, à minha madrinha, tio Tony e tia Fernanda.

Ao meu namorado Fábio, meu melhor amigo, meu apoio, pela motivação que és, pela força, paciência, dedicação e pelo amor.

Ao meu irmão Rui, pela admiração, por tudo o que significas para mim.

Aos meus pais, Pedro Pinto e Emília Dias, que permitiram a minha caminhada até aqui e tornaram possível a minha formação. Pela dedicação, esforço e por acreditarem em mim.

Index

Index of Figures

Index of Tables

List of Abbreviations

ABCB1 – ATP-binding cassette sub-family B member 1

ASCT - autologous stem cell transplantation

BAFF – B-cell activating factor

BCl-X_L – anti-apoptotic protein

bFGF – basic fibroblast growth factor

BM – bone marrow

BMECs – bone marrow endothelial cells

BMSCs – bone marrow stromal cells

CAM-DR – cell adhesion-mediated drug resistance

CCND1 – cyclin D1 gene

CCND2 – cyclin D2 gene

CCDN3 – cyclin D3 gene

CDKN2A – cyclin-dependent kinase inhibitors 2A

CRAB – Calcium elevation, renal insufficiency, anemia, bone abnormalities

CSC – cancer stem cell

ECM – extracellular matrix

EVs – extracellular vesicles

FGF – fibroblast growth factor

FGFR-3 - fibroblast growth factor receptor 3

HSCs – hematopoietic stem cells

ICAM1 – intercellular adhesion molecule 1

IFN-γ – interferon gamma

Ig – immunoglobulin

IGF-1 – insulin-like growth factor 1

IgH – immunoglobulin heavy chain

IgL - immunoglobulin light chain

IκB – inhibitor kappa B

IL – interleukin

LFA1 – lymphocyte function-associated antigen 1

IMiDs – immunomodulatory drugs

JAK/STAT3 – Janus kinase (JAK)–signal transducer and activator of transcription 3 (STAT3)

KRAS – RAS gene family member

MAF – transcription factor musculoaponeurotic fibrosarcoma

MAFB – transcription factor musculoaponeurotic fibrosarcoma B

MAPK/ERK – mitogen-activated protein kinase/extracellular signal-regulated kinase

Mcl-1 – myeloid cell factor 1

MDR – multidrug resistance

MDR1 – multidrug resistance protein 1

MicroRNAs – miRs

MGUS – monoclonal gammopathy of undetermined significance

MM – multiple myeloma

MMSET – multiple myeloma SET

MVBs – multivesicular bodies

MVEs – multivesicular endosomes

NFκB – nuclear factor B

NK – natural killer cells

NRAS – RAS gene family member

P18/CDKN2C – cyclin-dependent kinase inhibitors 2C

PCs – plasma cells

PI3K/AKT – phosphatidylinositol 3-kinase (PI3K)–Akt

P-gp – P-glycoprotein

PTEN – tumor suppressor gene

RB1 – tumor suppressor gene

SDF1α – stromal cell-derived factor 1α

SFM-DR – soluble factor-mediated drug resistance

SMM – smoldering multiple myeloma

TNFα – tumor necrosis factor-α

TP53 – tumor suppressor p53

VAD – vincristine-adriamycin-high dose dexamethasone

VEGF – vascular endothelial growth factor

VCAM1 – vascular cell adhesion molecule 1

VLA4 – very late antigen 4

Abstract

Multiple myeloma (MM) is a plasma cell malignancy characterized by uncontrolled production of monoclonal immunoglobulins within the bone marrow. Despite the recent major treatment advances, obtained with the introduction of new therapeutic agents such as bortezomib and lenalidomide, drug resistance is a major obstacle to therapeutic success. Therefore, it is urgent to identify biomarkers of MM drug resistance.

Extracellular vesicles (EVs) (including microvesicles and exosomes) are released by various cell types, contributing to intercellular communication. Tumor cells such as MM cells also release EVs, whose cargo may be transferred into recipient cells. Importantly, the presence of markers in the circulating EVs shed by tumor drug resistant cells, including particular microRNAs such as miR-21, may allow the detection of biomarkers of drug resistance.

Therefore, this study aimed at selecting a method and optimizing a protocol for the isolation of EVs with different sizes (possibly exosomes and microvesicles) from plasma samples of MM patients. Thus, a comparison of methods was carried out, including ultracentrifugation, a commercial kit (ExoQuick) and qEV size exclusion chromatography (SEC) columns. The isolated EVs were characterized in terms of size and purity, by dynamic light scattering (DLS) and transmission electron microscopy (TEM), respectively. In addition, the analysis of EV markers such as Hsp70, CD63 and CD9 was also carried out (by Western Blot), together with the detection of possible cellular contaminants and protein contaminants from the plasma. Finally, the expression levels of miR-21 and miR-16 was attempted (by qRT-PCR).

All the three methods allowed the isolation of EVs, but with distinct sizes. The ultracentrifugation allowed the isolation of EVs together with contaminants (possibly lipoproteins). In addition, this protocol had the disadvantage of requiring an expensive equipment (ultracentrifuge) and taking several hours. Moreover, the amount of total protein recovered from the ultracentrifugation protocol was very low. The ExoQuick kit allowed higher yields of total protein to be recovered from the isolated EVs and it was a much quicker protocol than the ultracentrifugation one; however, it only isolated the smaller vesicles (possibly exosomes). The qEV SEC columns were the preferred approach, since they enabled a rapid isolation of EVs with various sizes (possibly

exosomes and microvesicles). In addition, by pooling the various fractions collected, it is possible to have enough protein to be analysed by Western blot.

Finally, preliminary results indicate that RNAse treatment is necessary when analysing miRs from EV samples. In addition, when pre-treating samples with RNase, the three protocols seem to allow detecting similar levels of miRs. However, these preliminary results need to be confirmed before conclusions can be taken.

Keywords: cancer, multiple myeloma, cancer drug resistance or chemoresistance, extracellular vesicles, miRs

Resumo

O mieloma múltiplo é uma neoplasia maligna caracterizada pela produção descontrolada de imunoglobulinas monoclonais na medula óssea. Apesar dos recentes avanços nos tratamentos, obtidos sobretudo com a introdução de novos agentes terapêuticos como o bortezomib e a lenalidomida, a resistência aos fármacos continua a ser um dos maiores obstáculos para o sucesso terapêutico. Assim, é urgente identificar biomarcadores de resistência em mieloma múltiplo.

Vesículas extracelulares (incluindo microvesículas e exossomas) são libertadas por vários tipos celulares, contribuindo para a comunicação intercelular. Células tumorais de mieloma múltiplo também libertam essas vesículas extracelulares, que transportam no seu interior componentes que podem ser transferidos parar outras células. A presença de marcadores nas vesículas extracelulares circulantes no sangue, libertadas por células tumorais resistentes a fármacos, nomeadamente microRNAs como o miR-21, podem permitir a detecção de biomarcadores de resistência.

Assim, este projecto teve o objectivo de selecionar um método e optimizar um protocolo de extração de vesículas extracelulares com diferentes tamanhos (possivelmente exossomas e microvesículas) existentes no plasma de doentes com mieloma múltiplo. Para isso, foi realizada uma comparação entre métodos, incluindo a ultracentrifugação, um kit comercial (ExoQuick) e colunas de cromatografia de exclusão por tamanho (qEV). As vesículas extracelulares isoladas foram caracterizadas em termos de perfil de tamanho e pureza, respectivamente, por "Dynamic light scattering" (DLS) e por microscopia electrónica de transmissão (TEM). Além disso, a presença de marcadores como o Hsp70, CD63 e CD9 foi também analisada (por Western blot), bem como a presença de possíveis contaminantes celulares e proteicos com origem no plasma. Por fim, a expressão de miR-21 e miR-16 foi igualmente realizada (por qRT-PCR).

Os três métodos permitiram a extração de vesículas extracelulares, mas com diferentes tamanhos. A ultracentrifugação permitiu isolar vesículas extracelulares mas contendo contaminantes (possivelmente lipoproteínas). Este protocolo tem também as desvantagens de requerer equipamento dispendioso (ultracentrífuga) e de ser muito moroso. Além disso, a quantidade total de proteína conseguida com este método foi muito reduzida. Por sua vez, ExoQuick permitiu precipitar grandes quantidades de proteína total a partir de amostras de vesículas extracelulares, tendo sido ainda um protocolo muito mais

rápido em comparação com a ultracentrífugação; contudo, apenas permitiu isolar vesículas de pequenos tamanhos (possivelmente exossomas). As colunas de cromatografia qEV mostraram ser o protocolo preferido, uma vez que permitiram o rápido isolamento de vesículas extracelulares com diferentes tamanhos (possivelmente exossomas e microvesículas). Além disso, juntando as várias frações recolhidas das colunas qEV, é possível obter quantidade de proteína suficiente para ser analisada por Western blot.

Por fim, resultados preliminares indicaram que o tratamento com RNase é necessário para a análise de miRs a partir de amostras de vesículas extracelulares. Além disso, com o pré-tratamento das amostras com RNase, os três protocolos parecem permitir detectar quantidades semelhantes de miRs. Contudo, estes resultados preliminares precisam ser confirmados para que se possam retirar conclusões.

Palavras-chave: cancro, mieloma múltiplo, resistência aos fármacos, vesículas extracelulares, miRs

Chapter I - Introduction

INTRODUCTION

1. Multiple Myeloma

Multiple myeloma (MM) is a malignant blood disease that accounts for 1% of neoplastic diseases worldwide and 13% of all hematological cancers (Raab et al., 2009), being recognized as the second most common blood cancer (Mitsiades et al., 2004).

1.1. Pathogenesis

MM develops in the bone marrow (BM), being hallmarked by abnormal production of malignant plasma cells (PCs), proliferation of monoclonal immunoglobulin (Ig) in the blood or urine, and associated organ dysfunction (Mitsiades et al., 2004; Palumbo and Anderson, 2011), referred to as CRAB (hypercalcemia, renal insufficiency, anemia and bone lesions) (Rajkumar et al., 2014).

In healthy conditions, the PCs, which are derived from B-cells, are capable of producing normal IgM immunoglobulins to fight infections. This process includes maturation of B lymphocytes in the BM after expression of functional IgM, and migration to secondary lymph nodes, where B cells are presented to antigens in order to produce plasmablasts. The immature PCs or plasmablasts are typically short-lived cells involved in the primary immune response that usually produce IgM (Kuehl and Bergsagel, 2002; Seidl et al., 2003). However, in abnormal conditions, plasmablasts can undergo hypermutations of Ig light (IgL) and Ig heavy chains (IgH) variable genes, and secrete other Ig isotypes with high affinity, such as IgG and IgA, or rarely IgE and IgD (Seidl et al., 2003). These cells are then selected to survive and to migrate to the BM in order to differentiate into long-lived PCs for several days or even years (Kuehl and Bergsagel, 2002; Seidl et al., 2003). When abnormal monoclonal PCs start to proliferate and overproduce large amounts of immunoglobulins (Seidl et al., 2003) the disease develops **(Figure 1)**.

Hypermutations and aberrant isotype switching are primary genetic events for MM development and a major cause for translocations (Gabrea et al., 2006), but chromosomal abnormalities, mainly trisomies, are also seen in early stages of MM (Fonseca et al., 2004; Rajan and Rajkumar, 2015). Other aberrant genetic events occur

during MM development, such as mutations, deletion, methylations and microRNA (miRNA) abnormalities (Pandey MK, 2015).

From a genetic point of view, a first division can be made between: i) hyperdiploid karyotype, associated with numerous chromosomal anomalies (at chromossomes 3, 5, 7, 9, 11, 15, 19 and 21) but rare IgH translocations; and ii) non-hyperdiploid karyotypes, defined by the occurrence of several IgH translocations (Bergsagel and Kuehl, 2005; Mitsiades et al., 2004; Seidl et al., 2003).

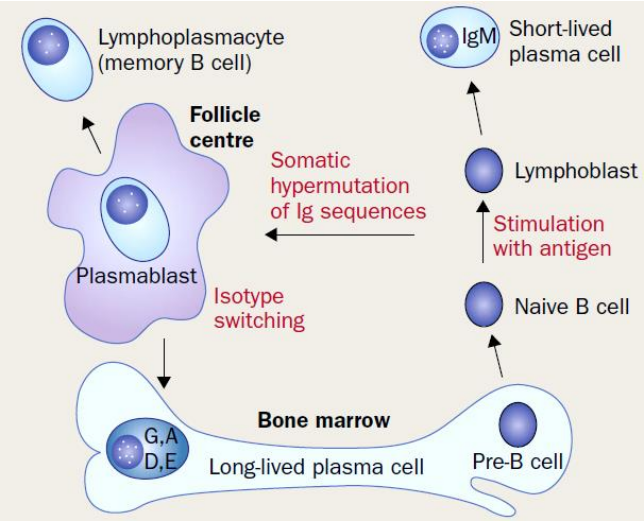

Figure 1. Multiple myeloma cells development in the bone marrow. Aberrant number of plasma cells after IgH switch recombination become more prone to survive and live in the bone marrow as totally differentiated and long-lived cells. As the number of plasma cells increases, the number of antibodies will be widely higher. Adapted from Seidl *et al*., 2003 (Seidl et al., 2003).

This neoplasia is frequently preceded by a condition designated monoclonal gammopathy of undetermined significance (MGUS), which denotes an excessive proliferation of PCs but relative stable levels of Ig protein (Alexander et al., 2007; Seidl et al., 2003) **(Figure 2)**. Patients at this stage of the disease do not suffer from symptoms but may later develop MM, at a rate of 1% per year at 20 years (Kyle and Rajkumar, 2008). In some cases, a MM premalignant stage has been recognized as smoldering multiple myeloma (SMM), more advanced than MGUS but also asymptomatic (Rajkumar, 2009). When symptoms appear the disease is termed as intramedullary or extramedullary MM, being the later more aggressive (Bergsagel and Kuehl, 2005). About

1 to 4% of all cases of MM progresses to a rare variant of the disease called plasma cell leukemia, a form of extramedullary MM with high levels of malignant plasma cells circulating in the peripheral blood and associated with a poor prognosis (Albarracin and Fonseca, 2011).

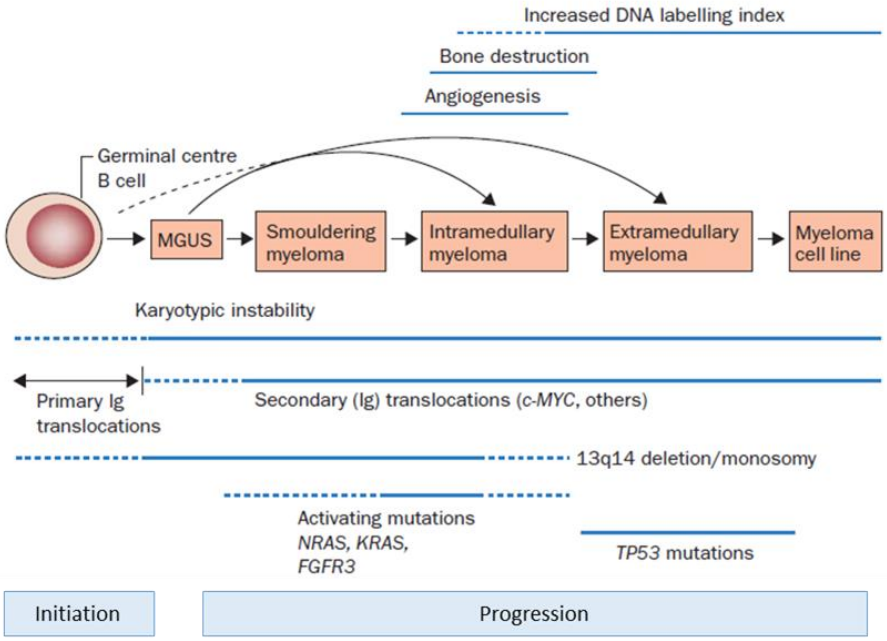

Figure 2. Multistep development for MM disease. Multiple oncogenic events such as chromosomal abnormalities and mutations occur in MGUS and other stages as the disease progresses. Adapted from Sirohi & Powles, 2004 (Sirohi and Powles, 2004).

The diagnosis of this disease occurs mostly in patients over 60 years old, between the average ages of 65 (Rajkumar, 2012) and 70 years old (Palumbo and Anderson, 2011). In the last years, the median overall survival increased to about 5 years, mainly due to the introduction of new therapeutic drugs, such as thalidomide, lenalidomide and bortezomib (Kumar et al., 2014).

1.2. Treatment

Overall treatments used for symptomatic MM comprise steroids, alkylating agents, glucocorticoids, anthracyclines, immunomodulatory drugs, proteasome inhibitors, monoclonal antibodies and autologous stem cell transplantation (ASCT) (Morgan et al., 2012). For decades, therapies were based on cytotoxic chemotherapy with

introduction of melphalan, an alkylating agent, and prednisone, a corticosteroid, which resulted in improved survival of patients (Kumar et al., 2008; Rajkumar, 2009). Later, high-dose chemotherapy with melphalan followed by ASCT was also introduced, resulting in higher overall survival compared with conventional chemotherapy (Kumar et al., 2008; Mitsiades et al., 2004). More recently, the introduction of new agents such as thalidomide, bortezomib and lenalidomide have increased the overall survival (Rajkumar, 2012). These facts are in accordance with studies that defined the median survival of 2,5 years prior to 1997, about 4 years in the following ten years (Kumar et al., 2008) and around 5 years in the recent years, due to the new therapies that have been introduced (Kumar et al., 2014; Rajkumar, 2011).

The choice of initial treatment has been changing over time. Patients are commonly stratified by age, performance status and comorbidities (Rajkumar, 2012), in order to decide if they are potential candidates for ASCT (Moreau et al., 2015; Rajkumar, 2011). Advanced age and vulnerability of patients are critical factors, since elderly patients have worse prognosis than those aged below 65 years old (Palumbo et al., 2011). Disease aggressiveness also helps to decide the best therapeutic approach. Standard MM patients have a better survival prognosis, from 6 to 7 years (Rajkumar, 2012). Patients with high risk myeloma with non-hyperdiploid karyotype, deletions of 17p or 13p chromosome, and translocations at t(14;16), t(14;20) usually are more intensively treated (Kyle and Rajkurnar, 2009; Rajkumar, 2012). The median overall survival of high risk MM patients is about 2-3 years, even with ASCT; therefore, for those patients, the main options are the novel therapies (Rajkumar, 2009).

For younger patients, high-dose treatment with melphalan followed by ASCT is the most appropriate approach (Moreau et al., 2015; San Miguel et al., 2008). These patients are usually treated with two to four cycles of induction therapy, which includes proteasome inhibitors and immunomodulatory drugs, before ASCT (Rajkumar, 2011). This first phase of treatment has the goal of reducing tumor burden in order to obtain better responses to the following treatments. It also improves the hematopoietic stem cell collection by decreasing PCs infiltration (Harousseau, 2012). Melphalan therapy is avoided once it can interfere with adequate stem-cell mobilization (Palumbo and Anderson, 2011; Rajkumar, 2011).

Elderly patients or those who are not eligible for ASCT can be treated with standard alkylating based therapy (Rajkumar, 2009). Over the years, the more common

treatment was oral combination of melphalan and prednisone, but currently they have been combined with thalidomide, lenalidomide or bortezomib (Harousseau et al., 2010; Rajkumar, 2009) with improved overall and progression free survival.

1.2.1. Bortezomib

Bortezomib was the first proteasome inhibitor approved as one of the new agents for the treatment of newly diagnosed MM patients and for relapsed and refractory MM (Anderson, 2005; Chen et al., 2011; Richardson et al., 2003).

Since aberrant proteasome activity seems to be important for the development of some malignancies, the introduction of proteasome inhibitors could prevent pro-apoptotic proteins degradation, resulting in apoptosis of malignant cells (Chen et al., 2011). Additionally, by inhibiting the degradation of IκB, which is the inhibitor of nuclear factor B (NFκB), bortezomib suppresses NFκB signaling pathway and prevents the activation of several anti-apoptotic genes that are important for MM progression (Chen et al., 2011; Richardson et al., 2003).

Another important mechanism of bortezomib as a proteasome inhibitor is through upregulation of NOXA, a pro-apoptotic member of the Bcl-2 protein family, which interacts with the anti-apoptotic proteins of the same family (the BCl-X_L and Bcl-2) and in this way induces apoptosis of the myeloma malignant cells (Chen et al., 2011). In addition, bortezomib is also used to treat bone disease because it inhibits osteoclasts and stimulates osteoblasts, thereby increasing bone formation (Mohty et al., 2014).

1.2.2. Thalidomide

Thalidomide is one of the immunomodulatory drugs (IMiDs) with several effects on the immune system. It modulates different components of the immune system to prevent the development of cancers by immune surveillance and by altering the inflammatory BM microenvironment which is important for MM development (Kotla et al., 2009). It seems that the benefits of thalidomide in MM are due to its ability of disturb the interactions between myeloma cells and the BM microenvironment (Anderson, 2005), e.g. by inhibiting interleukin-6 (IL-6), interleukin 1β (IL-1β), basic fibroblast growth factor (bFGF) and vascular endothelial growth factor (VEGF) expression, which are

important for the growth of myeloma cells (Anderson, 2005; Hideshima et al., 2000). The tumor necrosis factor-α (TNF-α), which is another cytokine important for MM cells growth and survival, is also affected by thalidomide (Hideshima et al., 2000). By decreasing the levels of this potent inflammatory cytokine, by modulating T cells, and by affecting other immune cells, thalidomide inhibits *de novo* IgM antibody synthesis (Kotla et al., 2009). Thalidomide also induces T-cell proliferation, by secreting interferon gamma (IFN-γ) and IL-2 (Hideshima et al., 2000; Kotla et al., 2009). However, thalidomide shows some side effects in patients such as deep vein thrombosis, constipation, peripheral neuropathy and fatigue. For that reason, safer analogues have been developed, such as lenalidomide (Richardson et al., 2009).

For many years, the molecular mechanism of action and targets of thalidomide and its derivatives, such as lenalidomide (see 1.2.3.), remained completely unknown. More recently, it was found that these IMiDs bound a primary target termed cereblon, which belongs to an E3 ubiquitin ligase complex. Initially, thalidomide action was related with direct inhibition of cereblon and, by consequence, with the inhibition of ubiquitination process, leading to the toxic accumulation of proteins and to MM cell death (Ito et al., 2010). However, novel findings associate cereblon with other downstream targets, supporting it as the main target for IMiDs. The cereblon protein has a role in binding, ubiquitination and degradation of Ikaros (IKZF1) and Aiolos (IKZF3), two transcription factors that maintain MM cells function (Kronke et al., 2014; Lu et al., 2014; Zhu et al., 2014).

1.2.3. Lenalidomide

In order for lenalidomide to act against MM, the presence of cereblon in cells is essential. In accordance to that, previous results have shown that, cells lacking cereblon become highly resistant to lenalidomide (Zhu et al., 2011).

Lenalidomide was proven to be more potent and effective than thalidomide, in modulating components of the immune system by immunomodulatory effects, altering several cytokines production, regulating T cell stimulation and increasing the natural killer (NK) cell cytotoxicity (Kotla et al., 2009).

Cytokines expression may be altered in neoplastic disease states. In MM, the secretion of these soluble proteins increases MM growth and survival and confers drug resistance (Hideshima et al., 2000; Kotla et al., 2009). Therefore, by acting as an immunomodulatory drug, lenalidomide inhibits the production of pro-inflammatory cytokines such as TNF-α, IL-1, IL-6, IL-12 and balances the production of anti-inflammatory cytokine IL-10 by increasing its levels (Kotla et al., 2009). Similarly to thalidomide, it inhibits MM cells and BMSCs binding and, consequently, decreases the production of IL-6, showing to be effective in downregulating TNF-α production by decreasing its levels up to 50,000 times more than thalidomide (Anderson, 2005; Kotla et al., 2009). It also decreases IL-6 directly, mediating the apoptosis of malignant myeloma cells and preventing their growth and proliferation (Kotla et al., 2009). Compared with thalidomide, it also co-stimulates about 50 to 2,000 times more T-cell proliferation triggered by T cell receptor, which is followed by an increased secretion, around 50 to 100 times higher, of IFN-γ and IL-2 (Anderson, 2005; Kotla et al., 2009). Besides the clonal production of both cytotoxic CD8+ and helper CD4+ T cells, it also enhances NK cell activity against MM cells without activating NK cells inappropriately (Anderson, 2005; Kotla et al., 2009; Lagrue et al., 2015).

Lenalidomide also blocks angiogenesis (being 2 to 3 times more potent than thalidomide as an antiangiogenic drug) by inhibiting the development of blood vessels required for the growth of primary and metastatic tumors, by decreasing the angiogenic factors VEGF and IL-6 (Kotla et al., 2009).

1.3. Causes of drug resistance in MM patients

MM patients successively relapse after one or more treatment regimens or become refractory (Yang et al., 2003). The major cause is drug resistance, which is dramatically associated with an unfavorable prognosis, reducing the chances for a successful treatment. In MM, drug resistance can be explained by 1) cytogenetic, genetic and epigenetic alterations, which occur during disease evolution contributing to MM pathogenesis (Abdi et al., 2013; Pandey MK, 2015); 2) abnormal drug transport and metabolism, that decreases the intracellular levels of drugs (Abraham et al., 2015); 3) deregulation of apoptosis and other intracellular signaling pathways (Abdi et al., 2013; Yang et al., 2003); 4) cancer stem cells, which are insensitive to therapies and capable of initiating MM (Abdi et al., 2013; Franqui-Machin et al., 2015) and 5) tumor

microenvironment, explained by the dependence of MM cells on the components of BM microenvironment (Abdi et al., 2013; Sirohi and Powles, 2004).

Cancer drug resistance may be due to intrinsic mechanisms, in which case malignant cells are resistant to therapies even before treatment initiation. Alternatively, drug resistance may be acquired during treatment, due to mechanisms acquired during the "selective pressure" of the drug treatment (Hideshima et al., 2007).

It is still not fully understood why patients relapse so frequently and how drug resistant MM clones alter their dominance and persist after therapies (Keats et al., 2012). However, due to the heterogeneous nature of MM, there are many causes involved in drug resistance **(Figure 3)**.

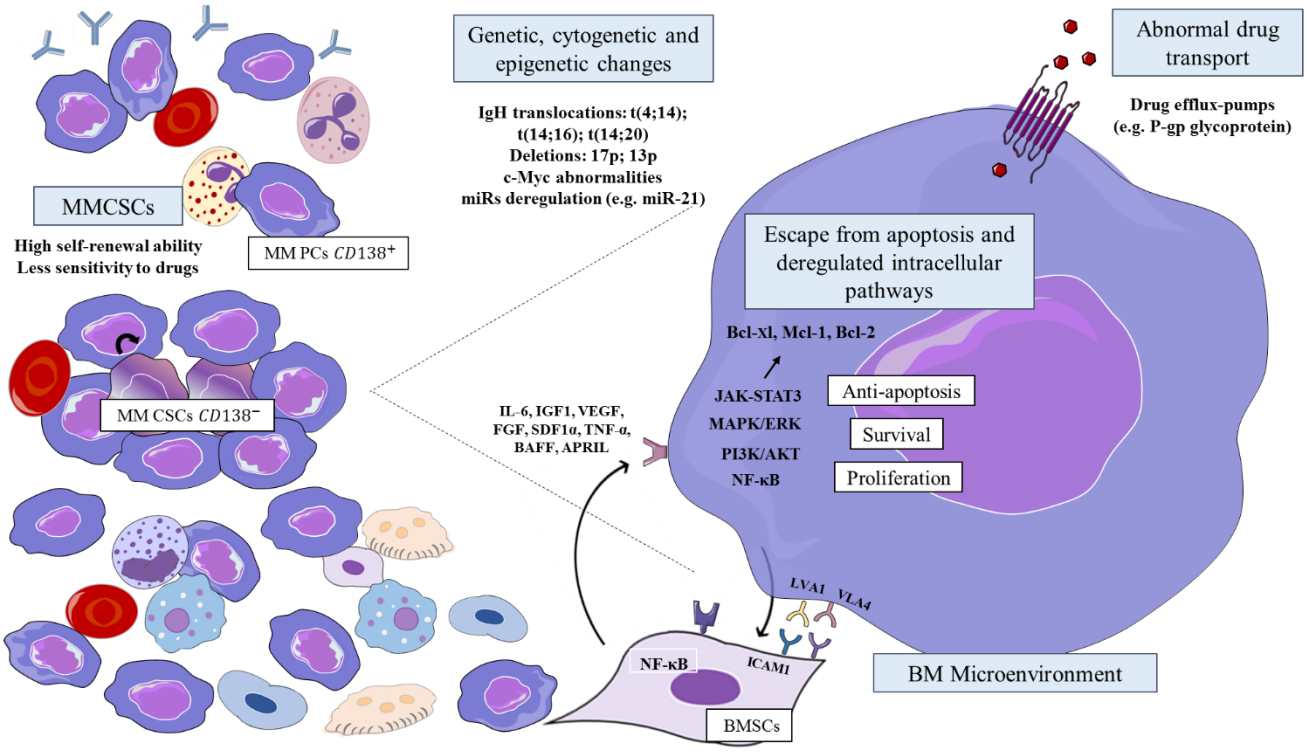

Figure 3 - Major causes of drug resistance in MM: (1) Of all the genetic, cytogenetic and epigenetic changes, the ones that are associated with an unfavorable prognosis are the t(4;14), t(14;16) and t(14;20) translocations, 17p and 13 p deletions and c-Myc associated abnormalities; (2) Drug efflux pumps, namely P-gp, mediate the efflux of several drugs to the outside of cells; (3) NF-κB, PI3K/AKT, MAPK/ERK and JAK/STAT3 are key signaling pathways involved in apoptosis and MM pathogenesis; (4) The cancer stem cell model postulates that, within the tumor, there are insensitive cells that, after exposure to the drugs, are capable of surviving and repopulating the

tumor (5) Bone marrow microenvironment plays an important role in MM survival, development and drug resistance by secretion of soluble factors e.g. interleukin 6 (IL-6), insulin-like growth factor 1 (IGF-1), vascular endothelial growth factor (VEGF), B-cell activating factor (BAFF), fibroblast growth factor (FGF), stromal cell-derived factor 1α (SDF1α), and tumor necrosis factor-α (TNF-α).

1.3.1. Cytogenetic, genetic and epigenetic alterations

Genetic, cytogenetic and epigenetic changes contribute to MM development and are correlated with predisposition to drug resistance and relapse (Pandey MK, 2015).

As mentioned above, IgH translocations and chromosomal abnormalities are the main alterations found in early stages in MM (Fonseca et al., 2004; Rajan and Rajkumar, 2015). In hyperdiploid patients IgH translocations are rare and usually these patients have better overall survival (Bergsagel and Kuehl, 2005). However, in non-hyperdiploid patients (55-70% of the cases), the initial genetic event is often an IgH translocation on chromosome 14q32 (Smadja et al., 2001; Talley et al., 2015). The most common partners are: 4p16.3, which is thought to result in upregulation of fibroblast growth factor receptor 3 (FGFR-3) and multiple myeloma SET domain (MMSET) genes; 11q13 that deregulates cyclin D1 gene (CCND1); 16q23 which upregulates the transcription factor musculoaponeurotic fibrosarcoma (MAF) and, consequently cyclin D2 gene (CCND2); 6p21 responsible for upregulation of cyclin D3 gene (CCND3); and 20q11, which mediates transcription factor musculoaponeurotic fibrosarcoma B (MAFB) levels (Seidl et al., 2003; Talley et al., 2015). Such translocations usually juxtapose Ig gene enhancers next to oncogenes (Mitsiades et al., 2004). The resultant unbalanced expression of the mentioned genes will contribute to the malignant phenotype of MM. Deletions and duplications, involving 1p, 1q, 9q, 11q, 12p, 13q, 15q, 16q, 17p, 19q and 22q chromosomes, are also frequent in non-hyperdiploid patients (Talley et al., 2015).

The t(4;14) translocations, occurring in 15% of patients, contribute to therapeutic failure and consequently to relapse, even when patients are receiving high dose drug therapy followed by stem cell transplantation (Gertz et al., 2005; Kalff & Spencer, 2012; Bergsagel et al., 2013). Treatment failures are mainly due to the overexpression of FGFR3 and MMSET genes (Chesi et al., 1998), both present in MM cells with the t(4;14) translocation and proven to be oncogenes (Chesi et al., 2001; Brito et al., 2009). FGFR3

is overexpressed in 74% of patients with t(4;14) translocations, while MMSET is overexpressed in all patients (Keats et al., 2012). Increased expression of the FGFR3 gene seems to contribute to tumor formation (Chesi et al., 1998), while the MMSET gene increases cell proliferation by decreasing cell cycle arrest, apoptosis and enhancing cell adhesion (Brito et al., 2009).

The presence of t(14;16) or t(14;20), which are less frequent among patients (occurring in 5% and 2% of patients, respectively), represent an unfavorable prognosis in MM patients (Ross et al., 2010). MAF (also named c-maf) and MAFB are, respectively, the key oncogenes found dysregulated in MM cells with t(14;16) and t(14;20) translocations (Chesi et al., 1998; Hanamura et al., 2001; Boersma-Vreugdenhil et al., 2004). The translocation t(14;16) results in increased MAF levels but also includes indirect upregulation of CCND2 genes, which were proposed to select the PCs more receptive to proliferative stimuli and, by contributing for adhesion to the stroma, lead to tumor proliferation and survival (Hurt et al., 2004). Nonetheless, the effect of enhanced MAFB levels in MM cells has to be further clarified (Hanamura et al., 2001; Boersma-Vreugdenhil et al., 2004).

The identification of t(11;14) and t(6;14) translocations allows the classification of MM patients as “standard risk” patients, since they lack outcome significance (Bergsagel et al., 2013). Among the IgH translocations, the t(11;14) is one of the most recurrent, appearing in 15 % of patients, while the t(6;14) is less frequent, associated with only 3 % of MM patients (Talley et al., 2015). Patients with the t(11;14) translocation normally have a good prognosis, since a study has shown that they respond equally to treatment using HDT and stem cell transplantation when compared to patients without the translocation (Gertz et al., 2005). Moreover, the t(11;14) upregulates CCND1, resulting in better overall response to bortezomib therapy (Ngo et al., 2010). However, some authors claim that CCND1 upregulation is related to bad prognosis and MM progression, since the CCND1 amplification is associated with increased MDR1 gene expression and chemoresistance (Sewify et al., 2014). The translocation t(6;14) influences CCND3 expression which, similarly to CCND1, regulates the cell cycle (Shaughnessy et al., 2001).

Deletion of 17p is strongly associated with advanced stages of MM and with drug resistance (Elnenaei et al., 2003). This 17p deletion is one of the most aggressive alterations, with bad prognosis, mostly due to a strong correlation with mutations of the

tumor protein p53 (TP53) suppressor gene (Lodé et al., 2010; Talley et al., 2015). Even treatments with HDT followed by stem cell transplantation (Gertz et al., 2005), lenalidomide (Reece et al., 2009), bortezomib (Avet-Loiseau et al., 2002) or thalidomide have failed in patients with this deletion, because the p53 function (in controlling the cell cycle and apoptosis) is deregulated (Boyd et al., 2011; Bergsagel et al., 2013). The same pattern occurs in relapsed or refractory patients (Dimopoulos et al., 2010), suggesting that 17p deletion negatively influences MM progression.

The most recurrent deleted chromosomal region found in MM is chromosome 13q, being identified in 43% of the patients and causing inactivation of the RB1 gene (Avet-Loiseau et al., 2002). This 13q deletion is associated with poor prognosis, mainly due to its correlation with t(4;14) and t(14;16) translocations, in 85% and 92 % of patients respectively (Avet-Loiseau et al., 2002). Relapsed patients with deletion of 13q achieved a similar response to bortezomib therapy compared to those without 13q deletion, which proposes that these patients normally benefit from bortezomib treatments (Sagaster et al., 2007).

Abnormalities in both the short and long arms of chromosome 1, respectively 1p deletion and 1q duplication, have been associated with shorter survival in MM (Talley et al., 2015). Patients carrying 1p deletion treated with HDT followed by ASCT were associated with reduced overall survival and remission (Qazilbash et al., 2007). Target genes implicated in 1p deletion are FAM46C and CDKN2C (Boyd et al., 2011). Gain in 1q chromosome also affects the outcome of patients that underwent the HDT followed by ASCT (Nemec et al., 2010) or a bortezomib-based therapy (since 1q gain may confer bortezomib resistance). Nonetheless, response rates to thalidomide are independent of 1q duplications (An et al., 2014).

Secondary translocations occur at a later stage and include overexpression of MYC oncogene at the 8q24 chromosome. Due to its colocalization with super-enhancers (Walker et al., 2014), MYC abnormalities are associated with disease aggressiveness and resistance to melphalan (Greco et al., 2006), and even bortezomib failed to improve survival of these patients (Sekiguchi et al., 2014).

Additionally, gene mutations involving, for instance, NRAS and KRAS, FGFR3 and TP53, p18/CDKN2C, CDKN2A and PTEN deletion or inactivation are found in MM

aggressive stages, playing a major role in oncogenesis by promoting tumor progression and drug resistance (Mitsiades et al., 2004).

Various epigenetic events were also associated to development and progression of this disorder (Seidl et al., 2003): i) global DNA hypomethylation and specific gene hypermethylation, which alter the expression of important genes; ii) aberrant histone modifications, which can promote cell survival and cell cycle progression and; iii) miRs deregulation, which affects several pathways involved in MM pathogenesis (Morgan et al., 2012).

1.3.1.1 MicroRNAs responsible for drug resistance in MM

In general, several miRs targeting important genes have been found deregulated in MM (Bi and Chng, 2014; Dimopoulos et al., 2013; Rocci et al., 2014). MiR-106-25 cluster is found upregulated in MM, favoring oncogenesis because of their capacity of this cluster to downregulate a positive regulator of p53 tumor suppressor. On the other hand, miR-15a/miR-16 were found downregulated in malignant cells compared with healthy plasma cells. In normal conditions they have a protective function in MM, acting as tumor suppressor miRs, for instance by inhibiting the NF-kB pathway or decreasing VEGF secretion, having an antiangiogenic activity and regulating tumor proliferation (Bi and Chng, 2014; Dimopoulos et al., 2013; Rocci et al., 2014).

Despite the identification of several deregulated miRs in MM, few have been described with a role in drug resistance. In this field of research, the most interesting studies have focused on miR-21 upregulation, which has been related with resistance to melphalan, dexamethasone and doxorubicin in MM cells. MiR-21 was found specially upregulated in MM cells when bound to BMSCs, showing the importance of the microenvironment in cell adhesion mediated drug resistance (CAM-DR) (Wang et al., 2011). These results are consistent with previous studies that found that miR-21 is upregulated in the presence of IL-6 and through the activation of STAT3 pathway (Löffler et al., 2007). Conversely, miR-21 by decreasing PTEN, one of its tumor suppressor's targets, upregulates the activity of phosphatidylinositol 3-kinase (PI3K)–Akt (PI3K/AKT) and mitogen-activated protein kinase (MAPK/ERK) pathways, increasing cell survival and drug resistance (Leone et al., 2013). Another study compared the expression of miRNAs between MM resistant cell lines and the respective parental cells, and found miR-21 and

miR-181a/b upregulated in the doxorubicin or melphalan-resistant ones (Bi and Chng, 2014; Dimopoulos et al., 2013). Other studies showed that miR-130b and miR-125b cause resistance to dexamethasone, contributing to decreased MM apoptosis (Bi and Chng, 2014). As previously stated, miR-15a acts as a tumor suppressor and its downregulation leads to increased resistance to bortezomib and melphalan in MM cells co-cultured with BMSCs (Pichiorri et al., 2011). When cells are sensitive to those drugs, miR-15a expression levels are restored and MM cell death occurs (Dimopoulos et al., 2013). Mir-29b has the same tumor suppressor role, by inhibiting the anti-apoptotic gene myeloid cell factor 1 (Mcl-1), and its overexpression sensitizes MM cells to bortezomib and apoptosis. However, miR-29b was found downregulated in MM cells in the presence of BMSCs, once more proving the importance of the microenvironment in regulating miRs expression and promoting drug resistance of MM cells (Bi and Chng, 2014). Finally, miR-33b is also found inhibited in MM, and its upregulation by MLN2238 (a novel proteasome inhibitor) increased MM cells apoptosis and sensitivity to the MLN2238 treatment and, consequently, decreased tumor proliferation (Bi and Chng, 2014). All these miRs are potential targets to overcome drug resistance in MM, but more studies are needed to understand their functional role and affected pathways (Bi and Chng, 2014; Dimopoulos et al., 2013). Nevertheless, the mentioned studies have proved that miRs deregulation may contribute to the development of a drug resistant phenotype.

1.3.2. Abnormal drug transport

The most common cause of drug resistance in cancer is abnormal drug transport, leading to decreased intracellular drug levels. This may occur by overexpression of the MDR1 gene, which codes for a drug efflux pump, the P-glycoprotein 1 (P-gp, also known as MDR1 or ABCB1) (Gottesman, 2002). This MDR1 gene and respective protein expression was already detected in several tumors, including MM (Dalton, 1997).

P-gp, with 170 kD-molecular weight, was first discovered in a multidrug resistant cell line and named P-glycoprotein once can alter membrane permeability to drugs (Juliano and Ling, 1976). P-gp is an energy-dependent drug transporter capable of pumping, structurally and functionally, dissimilar cytotoxic drugs towards outside the cell (Gottesman, 2002; Nooter and Stoter, 1996). In this way, malignant cells may become

cross-resistant to several drugs and develop a multidrug resistance (MDR) phenotype (Gottesman, 2002).

In myeloma patients, increased P-gp levels detected after specific treatments (using vincristine and doxorubicin) might be an unfavorable prognostic factor, predicting MDR and cancer relapse. These refractory patients showed significantly increased P-gp levels while the non-treated MM patients had a low P-gp expression (Grogan et al., 1993; Nooter and Sonneveld, 1994). However, increased expression of P-gp is not the exclusive reason to multidrug resistance, since other drug efflux pumps may be overexpressed by tumor cells, such as MDR-associated protein 1 (MRP1, also known as ABCC1) and breast cancer resistance protein (BCRP, also known as ABCG2). MDR is often associated with the overexpression of this three members of ABC (ATP-binding cassette) transporters superfamily (Tamaki et al., 2011). Despite this, only low levels of MRP mRNA were found in MM (Nooter and Stoter, 1996) and BCRP mRNA and protein levels were increased after treatments and doxorubicin (Turner et al., 2006). Several drugs were described as P-gp substrates in MM, namely, vincristine, doxorubicin (Grogan et al., 1993), dexamethasone, carfilzomib, melphalan and lenalidomide (Abraham et al., 2015). After receiving treatment with these drugs, majority of patients showed P-gp overexpression, except for those treated with melphalan. Thalidomide and bortezomib were described as poor P-gp substrates, decreasing their expression (Abraham et al., 2015). However, other studies indicate that bortezomib also interacts with P-gp reducing its function and expression (O'Connor et al., 2013).

In order to circumvent MDR mediated by P-gp overexpression, chemosensitizers were introduced to potentiate chemotherapy. These agents are used to inhibit, modulate or reverse the P-gp activity, since at high concentrations they compete for P-gp transport (Thomas and Coley, 2003). The first modulator tested was verapamil, in 1981, when its addition to leukemic sensitive and resistant cell lines resulted in increased cytotoxic effect of drugs, which was possibly explained by its ability to inhibit drug efflux pumps (Tsuruo et al., 1981). However, first MDR modulators were usually extremely toxic. As verapamil, another compound included in “first generation” modulators was cyclosporin, whose analogue PSC-833, a “second generation” agent, had high activity but still produced toxic effects (Thomas and Coley, 2003).

1.3.3. Escape from apoptosis and deregulated intracellular signaling pathways

Other known mechanism of drug resistance in MM patients is protection from drug-induced apoptosis (Yang et al., 2003). Apoptosis is a mechanism of programed cell death mediated by proteins and major signaling pathways, such as the NFκB, PI3K/AKT pathway and the proteasome pathway (Ghobrial et al., 2005). The MAPK/ERK and the Janus kinase-signal transducer and activator of transcription 3 (JAK/STAT3) pathways activated by IL-6 are also crucial for the induction of MM cellular apoptosis (Yang et al., 2003). MAPK/ERK and PI3/AKT pathways can also be activated by VEGF, FGF, stromal cell-derived factor 1α (SDF1α) (Lentzsch et al., 2004) or insulin-like growth factor 1 (IGF-1) (Ge & Rudikoff, 2000), which also activates PI3/AKT signaling pathway (Tu et al., 2000).

The Apo2L/TRAIL has been shown to induce apoptosis of MM cell lines and human cells that were resistant to dexamethasone, doxorubicin, melphalan and mitoxantrane (Mitsiades et al., 2001). Moreover, it reverted bortezomib-resistance of MM cells by increasing apoptosis (Balsas et al., 2009).

Among the pro-survival proteins, Mcl-1 has been shown to exert an essential effect, being correlated with MM cell survival, since its inhibition rapidly induced apoptosis (Zhang et al, 2002; Le Gouill et al., 2004 a). Mcl-1 expression was also evaluated in MM patients in distinct stages of the disease, confirming Mcl-1 overexpression and association with cancer relapse and disease severity (Wuilleme-Toumi et al, 2005). Mcl-1 levels were found increased in response to IL-6 (Zhang et al., 2002; Jourdan et al., 2003), following activation of the JAK/STAT3 pathway (Puthier et al., 1999), and also in the presence of VEGF (Le Gouill et al., 2004 b).

Increased expression of Bcl-2 proteins, associated with decreased Bax expression, were also correlated with MM malignant phenotype in some MM cells lines and primary MM cells (Spets et al., 2002). High levels of the Bcl-X_L protein contributed to the inhibition of apoptosis by activation of the JAK/STAT3 pathway by IL-6 (Catlett-Falcone et al., 1999; Guo et al., 2012). Therefore, Bcl-X_L expression is also correlated with MM drug resistance, being found at higher levels in relapsed patients when compared to newly diagnosed ones (Tu et al., 1998). Taking this into account, small Bcl-2 family inhibitors, which are BH3 mimetic molecules, have been tested in order to overcome resistance

conferred by anti-apoptotic proteins such as Bcl-2 or Bcl-XL. These BH3 mimetics have potential anticancer effect since they bind to Bcl-2 family members, allowing Bax and Bak to be free to induce apoptosis (Adams & Cory, 2007).

NFκB activation is essential in MM pathogenesis since it has a role both in BMSCs and MM cells (Hideshima et al., 2002). NFκB, which includes a family of five transcription factors, is widely known for its anti-apoptotic effects in MM, contributing to MM cells survival. Indeed, in myeloma cell lines and patient's samples, NFκB has been found constitutively active (Ni et al., 2001). Additionally, drug-sensitive MM cells show lower NFκB activity than drug-resistant ones, and NFκB levels are elevated in MM cells derived from relapsed patients (Chen et al., 2011). Thus, the NFκB blockage has been tested in several studies, for instance, by using thalidomide, arsenic trioxide and proteasome inhibitors such as bortezomib (Hideshima et al., 2001; Hideshima et al., 2002) or inhibitor kappa B (IκB) kinase inhibitors, which induced apoptosis of MM cells (Ni et al., 2001).

More recently, heat shock protein 90 (HSP90) has been associated with MM survival pathways. In particular, HSP90 stabilizes proteins involved in anti-apoptotic signals such as AKT, STAT3 and IL-6 receptors (Zhang et al., 2014), thereby causing activation of PI3/AKT, JAK/STAT3, MAPK/ERK (Richardson et al., 2011) and NF-κβ signaling pathways (Zhang et al., 2014). Conversely, Hsp90 has been previously described as a target of the JAK/STAT3, MAPK/ERK (Chatterjee et al., 2007), and also, through HSP70 expression, of the PI3K/AKT signaling pathways (Chatterjee et al., 2013). Taking these facts into account, Hsp90 inhibitors have been develop and also combined, for instance, with bortezomib (Ishii et al., 2012; Khong and Spencer, 2011; Mitsiades et al., 2006) or with specific inhibitors of major survival pathways for consequent activation of apoptosis (Chatterjee et al., 2013; Huston et al., 2008).

1.3.4. Cancer Stem Cells

The cancer stem cell (CSC) hypothesis may be a possible explanation for the high rates of relapsed MM patients (Agarwal and Matsui, 2010). According to this hypothesis, within the tumor there are different populations of cells with distinct sensitivities to chemotherapy, being the CSCs (or initiating cells) the insensitive ones (due to their potential for self-renewal, differentiation and remaining quiescent) (Abdi et al., 2013).

Evidence for the existence of CSCs in MM was produced in 1971, when it was possible to grow tumor stem cells colonies from mouse transplanted with MM cells (Park et al., 1971), and later, in 1977, from human MM stem cells (Hamburger and Salmon, 1977). Many years later, CSCs were identified in MM tumors (Matsui et al., 2004; Matsui et al., 2008).

The initial experiments demonstrated that $CD138^{+}$ PCs were more abundant, when compared to the ones that lacked CD138 expression, but had no clonogenic potencial. Moreover, $CD138^{+}$ MM cells had lower proliferative capacity, being originated by clonogenic $CD138^{-}$ B cells, which in turn were less sensitive to chemotherapeutic agent when compared to $CD138^{+}$. These clonogenic and resistant cells ($CD138^{-}$ MM cells) presented stem cell properties, e.g. increased levels of ALDH activity. Taking these findings into account, it was assumed that MM CSCs were derived from clonotypic B-cell populations, since B cells are capable of self-renewal and to produce clones during their development, giving rise to PCs. $CD138^{-}$ cells were also characterized phenotypically and found to have the same cell surface markers normally expressed on normal B cells: CD19, CD20 and CD27 (Matsui et al., 2004; Matsui et al., 2008). The same authors proved the highly clonogenic potential of $CD138^{-}$ MM cells, by reproducing the tumor and the disease in immunodeficient NOD/SCID mice. They also found that these clonogenic MM precursors are relatively resistant to dexamethasome, bortezomib and lenalidomide. Furthermore, they found that the same drugs inhibited $CD138^{+}$ cells growth (Matsui et al., 2008). In summary, it was suggested that clonotypic B cells are the CSCs in MM, since they share properties with normal stem cells, particularly self-renewal capacity and ability to give rise to differentiated cells, e.g. the PCs (Huff & Matsui, 2008; Ghosh and Matsui, 2009).

Some authors reinforced the idea that MM CSCs are part of a side population of cells, which are characterized by having a stem cell-like phenotype, with capacity to self-renew and being resistant to therapy. They also express increased levels of multidrug transporters, such as ABCG2/BCRP and ALDH1A1 enzymatic activity. In accordance to that, side population cells are associated with drug resistance and relapse, since they are frequently found in relapsed patients. However, there is no correlation between the existence of side population cells and $CD138^{-}$ cells. Actually, the side population is mainly associated with $CD138^{+}$ (Franqui-Machin et al., 2015; Saltarella et al., 2015). Therefore, the origin of CSCs in MM remains controversial (Basak & Carrier, 2010).

The characteristic pathways activated in CSCs (Hedgehog, Wnt and Notch) are considered highly activated in MM cells and are crucial for their development and maintenance (Agarwal & Matsui, 2010; Franqui-Machin et al., 2015; Saltarella et al., 2015). These pathways are activated mainly by autocrine signals and cytokines released from the BM microenvironment (Franqui-Machin et al., 2015). In MM, the Hedgehog pathway controls stem cell fate decisions, being active in a small fraction of cells, specifically in the $CD138^-$ cells. The inhibition of this pathway leads to the differentiation of these clonogenic cells (Peacock et al., 2006). It also mediates survival and desensitizes stem cells to drugs since it activates drug efflux pumps, such as the ABCG2 transporter (Franqui-Machin et al., 2015). The activation of the Wnt pathway and subsequent accumulation of β-catenin supports the proliferation of MM cells, as well as of hematopoietic stem cells, and therefore it may possibly be active in MM CSCs (Derksen et al., 2004). The Notch pathway contributes to MM survival and proliferation (Jundt et al., 2004). However, even though it was found highly expressed on the clonotypic B cells, the functional role of Notch on these cells remains undefined (Kellner et al., 2013).

Recently, a study pointed to BTK, a component found in B-cell receptors, as a promising therapeutic target, since it is located upstream of and mediates the Wnt and Akt pathways. Furthermore, BTK is absent in normal plasma cells while it is increasingly expressed (80%) in MM PCs. BTK also increases the levels of Nanog, a transcription factor that contributes to stemness in cancer cells (Franqui-Machin et al., 2015).

In summary, several authors believe that MM CSCs are the major cause for drug resistance and therapeutic failure. Therefore, a better understanding of their role and of the involved pathways is required (Huff & Matsui, 2008; Franqui-Machin et al., 2015).

1.3.5. Tumor microenvironment

The dependence of MM cells on the BM microenvironment also causes resistance to chemotherapy (Sirohi & Powles, 2004), named environment-mediated drug resistance (Abdi et al., 2013). Some authors divided this type of acquired resistance into two groups: soluble factor-mediated drug resistance (SFM-DR) and cell adhesion mediated drug resistance (CAM-DR). The first type includes all the cytokines and growth factors released into the bone marrow *milieu* and the second involves adhesion molecules (Meads

et al., 2009; Abdi et al., 2013). The last mechanism mentioned includes the adhesion of myeloma cells to stromal cells, such as fibroblast and other BMSCs or to extracellular matrix (ECM) components, such as fibronectin, involving tumor cell integrins (Sirohi & Powles, 2004; Meads et al., 2009; Abdi et al., 2013).

The BM microenvironment comprises not only the bone marrow stromal cells (BMSCs) and ECM proteins such as fibronectin, collagen, laminin and osteopontin, but also several cell components, hematopoietic stem cells (HSCs), progenitor and precursor cells, immune cells, erythrocytes, bone marrow endothelial cells (BMECs), osteoclasts and osteoblasts (Hideshima et al., 2007). The major soluble factors secreted include: IL-6, IGF-1, VEGF, B-cell activating factor (BAFF), fibroblast growth factor (FGF), SDF1α, and TNF-α (Seidl et al., 2003; Hideshima et al., 2007). All these factors are secreted reciprocally by interactions of myeloma cells with BMSCs and all of them are of huge importance to support survival (Seidl et al., 2003).

This crosstalk network between BMSCs and MM cells also activates signaling pathways, specifically the IL-6/JAK/STAT3 pathway (Catlett-Falcone et al., 1999; Puthier et al., 1999; Guo et al., 2012). Studies have shown that IL-6 is potentially involved in resistance to several chemotherapeutic drugs. For that reason, several inhibitors of the IL-6/JAK/STAT3 pathway have been developed in order to prevent MM proliferation and induce apoptosis. These inhibitors have shown (*in vitro* and in mouse xenograft models) positive effects when tested alone or combined with conventional therapies, such as dexamethasone (Burguer et al., 2009; Li et al., 2010), melphalan (Li et al., 2010; Hunsucker et al., 2011; Monaghan et al., 2011), bortezomib (Voorhees et al., 2007; Li et al., 2010; Monaghan et al., 2011) and lenalidomide (Lin et al., 2012).

Increased secretion of VEGF also enhances adhesion of MM cells and BMSCs. This adhesion of cells also increases IL-6 secretion by BMSCs, which in turn is capable of increasing the levels of VEGF secreted by myeloma cells (and vice-versa) (Podar et al., 2001). Increased VEGF levels in the microenvironment contributes to angiogenesis and to MM cell proliferation and migration (Podar et al., 2001; Seidl et al., 2003). Conversely, IL-6, VEGF and IGF-1, produced by BMECs, stimulate myeloma cells growth (Hideshima et al., 2007). Several VEGF inhibitors have been developed in order to circumvent MM proliferation, survival and associated drug resistance. These inhibitors contributed to increase MM cellular apoptosis in the presence of BMSCs by decreasing

IL-6 and VEGF secretion (Lin et al., 2002). Some inhibitors showed synergistic effects with melphalan and bortezomib (Podar et al., 2006).

Another cytokine, the TNF-α, regulates adhesion between MM cells and BMSCs by increasing the levels of lymphocyte function-associated antigen 1 (LFA1) and very late antigen 4 (VLA4) adhesion molecules or intercellular adhesion molecule 1 (ICAM1) and vascular cell adhesion molecule 1 (VCAM1), respectively, present in MM cells and BMSCs (Seidl et al., 2003; Hideshima et al., 2007). In a study using MM cell lines, the adhesion of MM cells, via VLA4 adhesion molecule, to the ECM component fibronectin prevented apoptosis and contributed to doxorubicin and melphalan resistance (Damiano et al., 1999).

The activity of NFκB is also important to induce drug resistance in myeloma cells since its activation regulates IL-6 secretion, which contributes to MM cells adhesion to BMSCs (Chauhan et al., 1996). Thus, by suppressing the NFκB signaling pathway, proteasome inhibitors were capable of inducing apoptosis (Ni et al., 2001). Bortezomib and thalidomide were capable of suppressing NFκB expression and of decreasing cytokines secretion in the BM milieu, inducing apoptosis of these malignant cells and overcoming drug resistance and the growth advantage of myeloma cells (Hideshima et al., 2001; Keifer et al., 2001).

In summary, the tumor microenvironment promotes MM cells growth, survival and migration, angiogenesis induction, cell immunity suppression and, by protecting the tumor from therapeutic interventions, contributes to the development of drug resistance (Hideshima et al., 2007).

2. Extracellular vesicles and their microRNA cargo as mediators of transfer of drug resistance from drug resistant to drug sensitive cells

Extracellular vesicles (EVs) are important mediators of intercellular communication, with both surrounding cells and distant cells from different tissues (Raposo & Stoorvogel, 2013). As they are secreted by all types of cells, they are involved in important physiological functions such as immune response (Nishida-Aoki & Ochiya et al., 2015). However, EVs are also released by tumor cells in order to transfer miRs and oncogenic proteins to recipient cells in the tumor microenvironment, contributing to tumor proliferation (Lee et al., 2012; Chen et al., 2012).

The encapsulation of miRs into EVs make them more stable and resistant to degradation by ribonucleases (Rocci et al., 2014). As they circulate inside vesicles in such a stable manner, they may be used as biomarkers in several cancers, since each tumor is characterized by a specific miR profile (Zhao et al., 2015). In addition, miRs contained in microvesicles and exosomes may function as signaling molecules with influence in targeted cells phenotype (Falcone et al., 2015). The expression of miRs found inside of EVs isolated from the plasma of healthy donors revealed that miRs have important functions as homeostasis regulators (Hunter et al., 2008).

For instance, EVs derived from breast cancer cells and glioblastoma carry elevated levels of miR-21 (a repressor of PTEN and PDCD4, important tumor suppressor genes), contributing to the development of the disease (Nishida-Aoki & Ochiya et al., 2015). The MDR protein may also be carried through these vesicles and incorporated into recipient (drug sensitive) cells, altering their phenotype by promoting drug efflux and tumor resistance of those recipient cells. Drugs can also be encapsulated into small vesicles and carried out of the donor cells (Zhao et al., 2015).

EVs can be isolated *in vivo* from several body fluids such as blood, semen, urine, bile, nasal fluid, faeces, amniotic fluid or cerebrospinal fluid (Raposo & Stoorvogel, 2013; Yáñez-Mó et al., 2015). They include exosomes and microvesicles, which differ mainly in their cellular origins and sizes. Exosomes are released by the fusion of multivesicular bodies (MVBs) or multivesicular endosomes (MVEs) with the plasma membrane and are 40–100 nm in size (Lee et al., 2012; Raposo & Stoorvogel, 2015). Microvesicles are released directly through budding of the plasma membrane and are generally larger, with 100–1,000 nm in size (Raposo & Stoovogel, 2013). EVs bind with

target cells and may be internalized by those cells. Two internalization mechanisms have been described, fusion and active endocytosis, both regulated by adhesion molecules present at the cell membrane and at the cell surface of EVs (Figure 7) (Minciacchi et al., 2015). Both exosomes and microvesicles have specific markers that may be surface markers such as tetraspanin proteins CD9, CD63, CD81 or internal markers such as Alix, flotilin-1 and Tsg101 (Lee et al., 2012; Zhang et al., 2015).

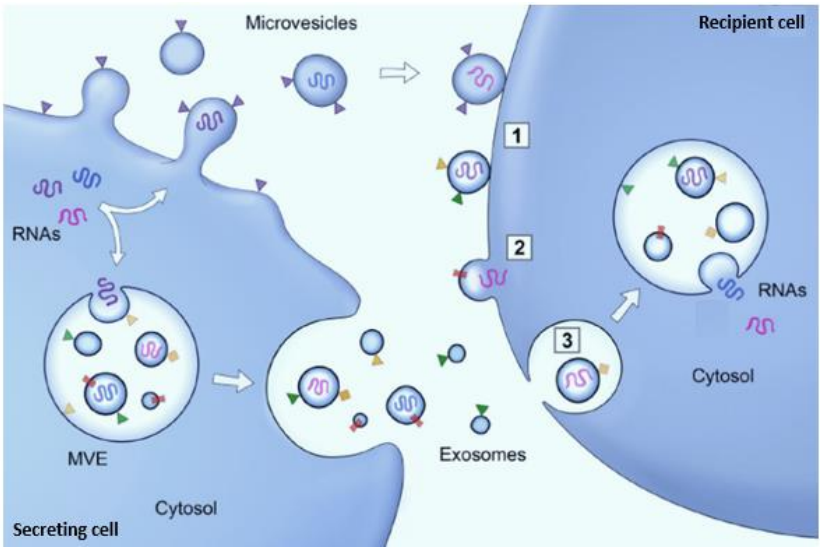

Figure 4. Horizontal transfer of proteins and RNA through EVs. Cargo from secreting cells is incorporated into MVs that directly bud from the plasma membrane, or into MVEs that fuse with the membrane to release exosomes. Microvesicles and exosomes dock at the plasma membrane of target cell (1) and fuse directly (2) or are endocytosed (3). Adapted from Raposo & Stoorvogel, 2013.

Some studies have already proved the importance of exosomes secretion to support MM development, as they found that both MM and BMSCs release, reciprocally, exosomes carrying different cytokines with a role in MM proliferation and drug resistance to bortezomib (Wang et al., 2014). Another study focused on the uptake by MM cells of exosomes containing miRs, released from BMSCs, to modulate genes expression in the MM cells. In this case, the authors found that miR-15a, a tumor suppressor miR, was downregulated in exosomes derived from BMSCs of MM patients, compared to normal patients, which facilitates progression of MM (Bianchi & Munchi 2015; Roccaro et al., 2013). This proves the important role of EVs and their content in the regulation of

tumorigenesis and drug sensitivity of MM cells. Neverthless, there is a lack of studies regarding the role of EVs in the transfer of information from resistant to sensitive MM cells.

As referred above, several miRs have been found deregulated in MM, some of them associated with drug resistance, but none has been described to be transported by EVs between resistant and sensitive MM cells. Actually, the association of EVs with drug resistance is a recent area of research. However, in breast cancer, it was already proved that resistant cells are able to release exosomes that alter the drug sensitivity of sensitive cells, partly due to the transfer of specific miRs associated with tumorigenesis and deregulated drug response. By quantitative real time PCR, it was suggested that miR-100, miR-222 and miR30a were mostly responsible for the observed increase in drug resistance in the recipient cells, since they were found upregulated in the EVs shed by the donor cells (Chen et al., 2014; Nishida-Aoki & Ochiya et al., 2015).

Therefore, studies are needed in order to detect a signature of specific miRs in EVs derived from resistant cells (compared to those derived from sensitive cells) and to understand which miRs function is related to the development of a drug resistant phenotype for a specific drug. Additionally, studies regarding the content of specific miRs, e.g. miR-21 or miR-15a (already associated with drug response and drug resistance in other cancers) in EVs shed by drug resistant MM cells should also be carried out. In this context, we propose to characterize EVs shed by MM cells in terms of size, specific markers of EVs and content in specific miRs previously known to be related with drug resistance.

Aims

The main goal of this project was to select and optimize a method for the simultaneous isolation of various types of EVs from the plasma samples of MM patients.

Therefore, the specific objectives of the present study were to:

- Isolate EVs from the plasma of MM patients with different methods: ultracentrifugation, a commercial kit (ExoQuick) and qEV size exclusion chromatography (SEC) columns;
- Characterize the size of the EVs obtained with the different methods and identify the ones which allowed the isolation of EVs with different sizes (presumably exosomes and microvesicles);
- Confirm that the isolates had EVs by analysing the expression of EV markers in the EV lysates from the three mentioned methods; In addition, check for possible cell contaminants and for protein contaminants from plasma.
- Initiate the study of the presence of specific miRNAs (miR-21 and miR-16) on the EVs isolated by the three methods.

With this work, it was expected to select a method and optimize the protocol, which could be used in future work, with the ultimate goal of identifying miRs as biomarkers of drug resistance in the circulating EVs from the plasma of MM patients.

Chapter II – Material and methods

2. Material and Methods

2.1. Cell lines maintenance

Human cell lines RPMI-8226 (peripheral blood, semi-adherent cells) and NCI-H929 (bone marrow, suspension cells) were purchased from DSMZ (Braunschweig, Germany). Cells were maintained in RPMI 1640 medium (Lonza) supplemented with 10% fetal bovine serum (FBS, Gibco) at 37ºC in a humidified atmosphere containing 5% CO_2. For the NCI-H929 cells, 50 µM of mercaptoethanol (Sigma-Aldrich) and 1mM of sodium pyruvate (Sigma-Aldrich) were added to the medium.

Cells were frequently observed using a light microscope and passaged every 2 to 3 days, when having reached about 80% confluency. Confluent NCI-H929 cells were passaged by diluting a volume of cells with fresh medium. To subculture RPMI-8226 cells, the medium containing free floating cells was first decanted and retained into a falcon tube. Then, cells were washed with a PBS solution (Sigma-Aldrich) and detached using a TrypLE Express reagent (Gibco), to dissociate the remaining cells after 3-5 min in the incubator. Once the adherent cells were transferred to the tube containing the free floating cells, they were centrifuged at 130 g (Centrifuge 5810R, Eppendorf) for 5 min and the resultant pellet resuspended in fresh medium.

Both cell lines were frequently counted using an hemocytometer and Trypan Blue (Sigma-Aldrich) in order to seed cells at a proper density (between 4-6 × 10^5 cells/ml) and to confirm cell viability values (typically over 70-90% for NCI-H929 cell line, and around 90% for RPMI-8226).

2.1.1. Cell lines genotyping and mycoplasma detection

RPMI-8226 and NCI-H929 cell lines were both genotyped and tested for mycoplasma presence. For this purpose, DNA extraction was performed. One T25 flask, for each cell line, was centrifuged for 5 min at 290 g (Centrifuge 5810R, Eppendorf) in order to obtain a cell pellet. Then, 1500 µL of a lysis buffer solution (Tris-HCl 1M, 1% NP-40, 1% SDS, pH 8.0) were added to the pellet and incubated for 1h at 65ºC. A solution of 5M NaCl (Sigma Aldrich), pre-heated at 65ºC, was added to the cell lysate. Afterwards, in order to precipitate and remove proteins, 2 mL of chloroform (Sigma-Aldrich) was added to the same solution. After 30 min of incubation at RT in a slow rocker, the mixture

was centrifuged at 1,200 g (Centrifuge 5810R, Eppendorf) for 10 min, at 4ºC. The upper aqueous phase was transferred to a new tube and the same volume of isopropanol (2-propanol, Merck Millipore) was added. The mixture was centrifuged at 17,000 g (Micro Star 17R, VWR) and the supernatant discarded. Pellet was washed with 1.5 mL of 70% Ethanol (Fischer Chemical) and then centrifuged at 17,000 g (Micro Star 17R, VWR) and the supernatant was discarded. The washing step was always performed twice with 70% ethanol. The DNA pellet was allowed to air-dry overnight and dissolved in 50 µl of ultrapure water. The DNA concentration was assessed using a NanoDrop 1000 Spectrophotometer (Thermo Scientific).

To test for the presence of mycoplasma, the commercial mycoplasma detection kit Venor®GeM Advance (Minerva Biolabs) was used. Then, 23 µl of the Rehydratation Buffer/Polymerase Mix were pipetted into PCR test tubes and 25 µl of the same mix into the positive control test tube. For the negative control, 2 µl of water was added to the respective reaction tube and, for each sample, 2 µl of DNA was pipetted into the tubes. After a brief spin, tubes were placed in a thermocycler with the following program:, 2 min at 94ºC for 1 cycle and 30 sec at 94ºC, 1 min at 55ºC and 30 sec at 72ºC for 39 cycles (MyCycler™ Personal Thermal Cycler, BioRad). The PCR products were analyzed on a standard agarose gel for the Genomics Core Facility.

The genotyping was performed on the DNA samples, by the IPATIMUP diagnostics, using the POWERPLEX 16 HS kit (Promega) for 15 STRs plus Amelogenin, in order to authenticate the source of the cells lines and to avoid possible cross-contamination with other cell lines.

2.2. Drugs

Bortezomib (BTZ, Selleckchem, Germany) and lenalidomide (LEN, Santa Cruz Biotechnology, California) were first dissolved in DMSO to a final concentration of 10 mM and 50 mM, respectively. Another stock solution of BTZ at 100 µM was prepared using the same solvent and frozen at -80ºC. Lower dilutions of BTZ and LEN were prepared in medium so that when they were added to the cells the final DMSO concentrations were always lower than 0,25%.

2.3. Selection of drug resistant cell lines and cell viability assays

Cell lines were cultured with stepwise increased concentration of BTZ. First, the half maximal inhibitory concentration (IC_{50}) of each drug was calculated in order to treat cells with a concentration near this value. NCI-H929 and RPMI-8226 cells were seeded, respectively, at a density of 15 x 10^3 and 10 x 10^3 cells per well (optimal concentrations previously determined) in 80 µL aliquots into 96 multi-well plate. Since drugs were dissolved in DMSO (Sigma-Aldrich), a control with the maximum DMSO concentration used was also included, to evaluate its effect on cells. After 24h, cells were treated with 10 µL of different BTZ and LEN concentrations. Ten µL of the PrestoBlue cell viability reagent (Invitrogen) were added to the cells 72 h after seeding, followed by a 20 min incubation at 37 ºC. Subsequently, the fluorescence values at 560-590 nm were measured, using a microplate reader (BioTek Synergy Mx) and the Gen5 software (BioTek). All experiments were done in triplicate and performed when cells had at least 90% viability.

During 6 months, fresh BTZ was added to cells every 3 to 4 days. Increasing concentrations were applied to cells. Cells that survived this treatment were named as resistant cells. Parental cells that did not receive any treatment were also maintained in culture in order to confirm that the passage number will not affect the results.

After 6 months, drug-response curves of the selected cells and of the parental ones were performed, with the Rezasurin assay. Cells were seeded in 96-well plates at optimal concentrations and incubated for 24 hours. Cells were then treated with serial dilutions of BTZ, ranging from IC_{50} to four times the IC_{50} value. Ten µL of Resazurin solution (1mg/mL) (Sigma-Aldrich) was added to each well and plates were then incubated at 37ºC for approximately 3.5 h. Resazurin is a blue non-fluorescent dye that is converted to resorufin only by enzymes present in metabolically active cells. Thus, the amount of highly fluorescent resorufin is then measured using a microplate reader (BioTek Synergy Mx) at 560-590 nm and using the Gen5 software (BioTek).

2.4. Preparation of plasma samples from blood of multiple myeloma patients

Human peripheral blood and bone marrow samples from 48 MM patients were obtained from Centro Hospitalar São João (Porto, Portugal), between September 2015 and July 2016. Peripheral blood and bone marrow samples were provided from cancer patients newly diagnosed or after receiving chemotherapy. The study was approved by

the São João Hospital's ethical review board and designed according to the tenets of the Declaration of Helsinki. Written informed consent was obtained from all participants.

Blood samples were collected in EDTA tubes (BD Vacutainer) and processed within 1h to 4h after collection. Samples were mixed with an equal volume of sterile PBS. For 4 ml of the blood and PBS mix, 3 ml of Ficoll were placed in a 15 ml centrifuge tube and then the blood and PBS were loaded carefully over the top of Ficoll. Samples were centrifuged at 400 g (Centrifuge 5810R, Eppendorf) for 30 min at 18-20 ºC (with the brake off). After the first spin, four different layers were visible; the upper layer (of plasma free of cells) was the layer of interest since it contained EVs. Plasma samples were aliquoted in 1.5 mL eppendorfs/vials and frozen at -80ºC.

Peripheral blood and bone marrow samples were also a source of lymphocytes which were present at the PBMCs and BMMCs layers respectively (which appear at the interface plasma/Ficoll). The lymphocyte layers were then transferred to a clean tube in order to wash cells with 3 volumes of PBS. After mixing and centrifuging at 90 g for 10 min (Centrifuge 5810R, Eppendorf), the supernatant was removed and this washing procedure was repeated. The resulting pellet was re-suspended in 1 mL of freezing media (10% DMSO, 90% FBS) and aliquots were frozen at -80ºC.

2.5. Extracellular vesicles isolation from plasma

2.5.1. **Ultracentrifugation**

EVs were isolated from plasma, by ultracentrifugation, using previously described methods, with some modifications (Caby et al., 2005; Théry et al. 2006; Khan, 2015). Frozen plasma was thawed, diluted in PBS (1 mL diluted in 9 mL of sterile PBS) and centrifuged. The first three centrifugations were for 10 min at 300 g, for 10 min at 2,000 *g* (Centrifuge 5810R, Eppendorf) and for 30 min at 10,000 g (Optima XE-100 Ultracentrifuge, Beckham Coulter) and were performed in order to pellet and remove cells, dead cells and cell debris, respectively. After each centrifugation, the supernatant was transferred into new tubes, without disturbing the pellet to avoid contamination. To collect the EVs fraction, supernatant was centrifuged overnight at 100,000 g (Optima XE-100 Ultracentrifuge, Beckham Coulter). After the centrifugation, the supernatant was poured off, the pellet was resuspended in PBS and, to wash the EVs, a new centrifugation

step was performed for 2 h at 100,000 g (Optima XE-100 Ultracentrifuge, Beckham Coulter). All the centrifugation steps were performed at 4ºC. The ultracentrifugation steps were carried out using the swinging-bucket rotor SW 32 Ti with the respective adaptors and 38.5 mL tubes (Ultra-Clear™, Beckman Coulter).

Following the last ultracentrifugation, the EVs were separated into two tubes for washing the EVs. The EVs from one tube were used for size determination, TEM and RNA extraction, while the EVs from the other tube were used for protein analysis. For size measurement, the resulting pellet was resuspended in 70 to 100 µL of PBS, of which 10 µL were saved for TEM analysis and the remaining 90 µL reused for RNA extraction. For Western blot analysis, the pellet was resuspended in 20 to 30 µl of lysis buffer and, following a final centrifugation at 16,200 g for 10 min at 4ºC (Micro Star 17R, VWR), the supernatant was collected and stored at -20ºC.

2.5.2. Exoquick kit (System BioSciences, SBI)

The ExoQuick™ protocol was carried out according to the manufacturer's instructions. Initially, 250 µL of plasma sample were treated with 2.5 µL of (500U/mL) human Thrombin (anti-coagulant, Sigma-Aldrich), to a final concentration of 5U per mL of plasma to remove fibrinogen. After a 5 min incubation and centrifugation at 9,600 g for additional 5 min (Micro Star 17R, VWR), the supernatant was collected to a new tube. Next, exosomes were precipitated by the addition of 63 µL of ExoQuick (System Biosciences) and incubated at 5ºC during 30 to 60 min. After centrifugation at 1,500 g for 30 min (Micro Star 17R, VWR), the exosomes were resuspended in 70 to 100 µl of PBS or 50 to 100 µL of lysis buffer for particle size analysis or Western Blot, respectively, as mentioned above.

2.5.3. qEV SEC columns (Izon Science)

Size exclusion chromatography (SEC) using commercial qEV columns was performed according to the manufacturer's instructions, with some modifications. Plasma samples (500 µL) from peripheral blood were loaded on the qEV SEC columns, with the lower-cap on. After removing the lower-cap, 0.5 mL fractions were collected. The first 3 mL (first six fractions) were discarded, and the vesicles fractions were immediately collected (fractions 7 to 12). During the process, and to avoid the column to run dry or

the unwanted dilution of the sample, small amounts of buffer (PBS) were added to the column top-filter. After collecting the fractions of interest, the columns were filled with at least 10 mL of PBS. The time needed for half of the volume to pass through the column was registered (before and after loading the sample) in order to control the flow rate and know when to clean the columns. The columns were then stored in the presence of a bacteriostatic agent (20% ethanol) at 4ºC. In some cases, fractions 7 to 12 were pooled for further size characterization, protein analysis and RNA extraction.

2.6. Trichloroacetic acid (TCA) precipitation

In order to precipitate proteins from each PBS solution which contained the EVs of interest, a TCA protocol was performed (provided by Baranyai et al., 2015) with minor modifications. Each diluted fraction isolated using qEV SEC columns was mixed with TCA to a final concentration of 20% TCA. After vortexing for 5 sec, the mixture was incubated on ice for 15 min. Then, a centrifugation at 14,000 g and 4ºC was performed during 15 min, and the supernatant removed. Pellets were dissolved in 20 to 100 µL of lysis buffer and in case of an hazy sample, 1-2 µL 1 M NaOH was added.

2.7. Dynamic Light Scattering (DLS)

The size of the EVs (isolated either with ultracentrifugation, Exoquick or qEV SEC columns) was measured using dynamic light scattering (DLS). A fraction of at least 70 µL of the EVs was resuspended in PBS, added to a polystyrene cuvette and used for immediate DLS analysis using the Zetasizer Nano ZS system and corresponding software (Malvern Instruments). Samples were allowed to equilibrate for 2 min and measurements were performed at a temperature of 25ºC.

2.8. Transmission electron microscopy (TEM)

Prepared EVs isolated with the three different methods (ultracentrifugation, Exoquick and qEV SEC columns) were analyzed by transmission electron microscopy (TEM). Briefly, 10-15 µL of the EVs resuspended in PBS were placed onto Formvar-carbon coated electron microscopy grids for 2 min and allowed to dry by using a filter paper. Grids were stained with uranyl acetate and observed in a transmission electron

microscope (Jeol JEM 1400) at an acceleration voltage of 80 kV. Data was obtained by the Histology and Electron Microscopy Service, IBMC/i3S, Porto.

2.9. Western Blot

EVs were resuspended and lysed in Winman's buffer (Tris-HCl 1 M pH 8.0, NaCl 5 M, EDTA 50 mM, 1% NP-40) or RIPA buffer (Tris-HCl 50mM pH 7.4, NaCl 150 mM, EDTA 2 mM, SDS 0.1%, NP-40 1%) with EDTA-free protease inhibitor cocktail (Roche). For the qEV SEC samples, a TCA protocol was used for protein precipitation and fractions were then lysed in RIPA buffer. Protein quantification was assessed by using a method based on the Lowry protocol (Bio-Rad DC™ Protein assay) and fluorescence was read in a microplate reader at 655 nm after 30 min incubation in the dark. Bovine serum albumin (BSA) was used to generate a standard curve.

Equal amount of protein was mixed with Laemmli buffer (Tris-HCl 1 M, 5% SDS, 12% Glicerol, 13% β-mercaptoethanol, 0.025% bromophenol blue) and boiled for 5 min at 95ºC. Proteins (2µg-10µg) were separated on a 12% Tris-glycine SDS-Page polyacrylamide gel for, at least, half an hour at 70 V followed by an hour at 100 V. A 12 % resolving gel (Tris-HCl 1.5 M pH 8.8, 30% Acrilamide, 10% SDS, 10% ammonium persulfate, TEMED) and a 5% stacking gel (Tris-HCl 1.0 M pH 6.8, 30% Acrilamide, 10% SDS, 10% ammonium persulfate, TEMED) were used. Running buffer was prepared from commercial 10X TGS solution (Bio-Rad). Proteins were transferred onto a nitrocellulose membrane Amersham Protran 0.45 NC (GE Healthcare) for 1 h at 100 V. Transfer buffer was prepared from the commercial 10X TG solution (Bio-Rad).

Membranes were blocked with 5% milk in Tris-buffered saline (TBS-T) solution with 0.1% Tween-20 (Promega) for at least 30 min with agitation and incubated with primary antibodies. After washes in TBS-T, membranes were incubated with secondary antibodies for 1h at RT. An ECL Western Blotting Detection Reagent (GE Healthcare), the chemiluminescence film Amersham Hyperfilm™ ECL (GE Healthcare) and the Kodak GBX developer and fixer (Sigma) were used for signal detection.

Commercial antibodies used for the Western blotting were the following: anti-CD63 (1:1000, SBI, EXOAB-CD63A-1) anti-Hsp70 (1:500, SBI, EXOAB-Hsp70A-1), anti-CD81 (1:500, SBI, EXOAB-CD81A-1), anti-CD9 (1:1000, SBI, EXOAB-CD9A-1), anti-Syntenin-1 (1:200, Santa Cruz Biotechnology, sc-100336), CHMP4B (1:100, Santa

Cruz Biotechnology, sc-82556), anti-ARF6 (1:100, Santa Cruz Biotechnology, sc-7971), anti-Actin (1:1000, Santa Cruz Biotechnology, sc-1616), anti-tubulin (1:10 000, T6074, Sigma Aldrich), anti-Cytochrome C (1:1000, Santa Cruz Biotechnoμogy, sc-13560) and anti-albumin (1:2000, Santa Cruz Biotechnology, sc-271605). All the antibodies were incubated at 4ºC overnight, with the exception of the anti-albumin which was incubated for 90 min.

2.10. RNA extraction

Total RNA extraction was performed using the miRCURY kit (Exiqon). Some samples were pre-treated with RNase A (Thermo Scientific). RNase A was added to the EVs isolates at a final concentration of 10 μg/mL and after a brief spin, the samples were incubated for 15 min at 37ºC.

Using the miRCURY kit, RNA was extracted from 100-200 μL of PBS solution containing EVs, following the manufacturer's instructions. Prior to start the lysis step, 10 μL of β-mercaptoethanol were added to each 1 mL of lysis solution. For each sample, 350 μL of lysis solution were added and samples were vortexed for 15 sec. Additionally, 200 μL of absolute ethanol was added and samples were vortexed for 10 sec. After the lysis step, total RNA purification was performed. For that purpose, columns provided by the kit were assembled and the total lysate with the ethanol applied onto the column, followed by 1 min centrifugation at 3,500 *g* (Micro Star 17R, VWR). The flowthrough was discarded and the column reassembled. Wash solution (400 μL) was applied to the columns, which were then centrifuged for 1 min at 14,000 *g* (Micro Star 17R, VWR). The washing was repeated twice by adding additional 400 μL of Wash Solution and by discarding the flowthrough between each wash step. Lastly, the column was centrifuged 2 min at 14,000 *g* (Micro Star 17R, VWR) in order to completely dry the resin. In order to elute the RNA, 50 μL of elution buffer was added to the column, which was followed by centrifugations at 200 *g* for 2 min and at 14,000 *g* for 1 min (Micro Star 17R, VWR).

Quantification of RNA was assessed using a NanoDrop™ 1000 Spectophotometer (Thermo Scientific). All the purified RNA samples were stored at -80ºC.

2.11. cDNA Synthesis by Reverse Transcription

Total RNA extracted from samples was used for cDNA synthesis using the miScript II RT Kit (Qiagen). For each experiment, a reverse-transcription master mix was prepared using 4 μL of 5x HiSpec Buffer, 2 μL of 10x miScript Nucleics Mix and 2 μL of miScript Reverse Transcriptase Mix. Variable volumes of RNAse free water and template RNA were added to each PCR tube, making up the final reaction volume to 20 μL. For the validation of this experiment, negative controls (with no sample or without the enzyme) were also used. Tubes were incubated for 60 min at 37ºC following additional 5 min at 95 ºC to inactivate the reverse transcriptase enzyme and holding at 4ºC in a thermocycler (MyCycler™ Personal Thermal Cycler, Bio-Rad). The tubes were then placed on ice or stored at -20ºC until further analysis.

2.12. Quantitative Real Time-PCR (qRT-PCR)

The synthesized cDNA was used for mature miR profiling by qRT-PCR using the SYBR Green PCR Master Mix (Qiagen). For each miR primer assay, a standard curve was prepared and all the RNA samples were run in duplicate. Briefly, 10 μL of 2x QuantiTect SYBR Green PCR Master Mix, 2 μL of 10x miScript Universal Primer, 2 μL of 10x miScript Primer assay (miR-21, miR-16 and U6) and 5 μL of RNase free water were added to each master mix. Then, 1 μL of template cDNA and 19 μL of the prepared master mix were pipetted to individual wells in 96-well plates, to a final volume of 20 μL. A standard curve was established by using serial dilutions of cDNA synthesized from RNA extracted from the RPMI-8226 cell line. Negative controls containing RNase free-water in place of the cDNA sample (NTC – no template control) were performed for each experiment. The plate was centrifuged for a split second. Afterwards, the template and the cycling program were made using the 7500 Software v2.0.6 (Applied Biosystems). The PCR amplification was conducted on a 7500 Fast Real-Time PCR System (Applied Biosystems) using the following program: 95ºC for 15 min for enzyme activation, followed by 40 cycles for denaturation of samples at 94ºC during 15 sec, annealing at 55ºC for 30 sec and for extension at 70 ºC for 30 sec. The results were analyzed using the same 7500 Software v2.0.6 (Applied Biosystems).

Chapter III – Results and Discussion

3. Results and Discussion - Part I

EVs present in plasma of cancer patients are potential biomarkers for diagnosis, prognosis and detection of drug resistance. Indeed, this is a promising area for the detection of biomarkers, since the cargo of the EVs is "protected" from plasmatic degradation. Nevertheless, the small size of the EVs makes it extremely difficult to isolate them from small plasma volumes. Some protocols have been recently developed and published but, being a relatively recent area of research, there is a need to optimize the existing isolation protocols in order to isolate EV without cellular or protein contaminants, with fast and reproducible protocols.

Recently, other studies have been conducted in order to compare methods/protocols and to optimize the isolation of EVs from human plasma, but particularly aiming only for exosomes isolation (Baranyai et al., 2015; Boing et al., 2014; Lobb et al., 2015; Muller et al., 2014). Indeed, the majority of studies rely on exosomes as possible biomarkers, overlooking the potential of the larger vesicles as carriers of important cellular information. Nevertheless, the smaller vesicles or exosomes (<100 nm) probably carry different information from the larger vesicles or microvesicles (100-1000 nm). Indeed, previous results from the Cancer Drug Resistance research group of i3S have shown for the first time that multidrug resistant cells shed more microvesicles than exosomes-like vesicles, when compared with their drug-sensitive counterpart cells (Lopes-Rodrigues et al., 2016). Moreover, the same study found differences in the protein content of the EVs produced by either multidrug resistant or sensitive cells.

Therefore, this study aimed to compare three distinct methodologies for the isolation of EVs from human MM plasma samples: the "standard" protocol of ultracentrifugation, the commercial ExoQuick kit (SBI) and a more recent method which is based on size exclusion chromatography separation by qEV SEC columns. The protocols here used were previously published but adapted in order to allow specific requirements: i) isolate all the EVs from the plasma samples and not only the exosomes (as most of the published protocols do); ii) if possible, separate the exosomes from the microvesicles; iii) use a maximum of 1250 µl of plasma; iv) isolate sufficient EVs to allow their characterization by size (by DLS and/or TEM) and molecular markers (by Western blot) and to allow detection of miRs (by qRT-PCR) and v) be as fast and economic as possible.

The three methods used were selected for being based on different approaches: centrifugation, precipitation and chromatography.

The ultracentrifugation (or differential centrifugation) is the most common method to isolate EVs (Momen-Heravi et al., 2012; Szatanek et al., 2015). The protocol includes a number of sequential centrifugations at different centrifugal forces (g). In the first three centrifugations, at 300 g for 10 min, 2,000 g for additional 10 min and 10,000 g for 30 min, the purpose is to get rid of the pellet that contains intact cells, dead cells and unwanted cell debris. Then, a final ultracentrifugation at 100,000 g for about 1 h aims to pellet the EVs. Some protocols have an additional last step at the same high speed, in order to wash EVs in a large volume of PBS. All the centrifugations are carried out at 4˚C (Szatanek et al., 2015; Thery et al., 2006). Nevertheless, this protocol has been optimized for the purification of exosomes (<100 nm) from conditioned cell culture media and, since the discovery of EVs in biological fluids, Théry et al. have proposed a new protocol with minor modifications. For instance, the initial sample should be diluted with equal volume of PBS, as body fluids are viscous. Because of that characteristic, the time and centrifugation speeds should also be increased (Caby et al., 2005; Khan et al., 2012; Thery et al., 2006). For that reason, the protocol used in this work has included an overnight centrifugation to pellet the EVs. Moreover, as the centrifugation steps between 12,000 to 15,000 g have the purpose of pelleting microvesicles, a centrifugation at 10,000 g was performed, to get rid of debris, followed by a centrifugation at 100,000 g overnight, to obtain microvesicles and exosomes in the same pellet. This was followed by an additional centrifugation for 2 h at the same high speed, for washing the EVs (Caby et al., 2005; Khan et al., 2012; Thery et al., 2006).

The ExoQuick™ kit is a proprietary precipitation reagent and polymer based (generally containing polyethylene glycol (PEG)), mainly used for exosomes precipitation. The precipitation solution is combined with the biofluid and, after an incubation at 4ºC, the mixture is centrifuged to form a visible pellet containing exosomes.

The qEV SEC columns are fundamentally based on the existence of columns with a stationary phase (normally a gel) and a mobile phase (normally a liquid) that allow particles elution and separation based on size. The larger vesicles will elute more rapidly, being collected in the initial fractions, while the small vesicles will take longer to elute since they can enter the stationary phase pores, being obtained in later fractions (Szatanek et al., 2015). Several studies were performed using sepharose home-made SEC columns

(Böing et al., 2014; Muller et al., 2014; Baranyai et al., 2015; Hong et al., 2016). However, in this study the commercial qEV SEC columns were used. Typically, after performing the qEV SEC columns protocol, and having obtained the EVs in a pellet, some authors centrifuged the collected fractions around 20,000 g (Sodar et al., 2016) or around 100,000 g for 1h or longer (Muller et al., 2014), in order to pellet the eluted EVs. Others have concentrated the EVs with Amicon® filters (Lobb et al., 2015). However, it was described that filtering the sample, e.g. forcing the passage of EVs through the filter, may damage the EVs force (Szatanek et al., 2015). Therefore, the more recent protocols perform SEC by gravity or by applying the smallest possible force. For that reason, in this work the samples were loaded into the columns and, after collecting the various fractions, it was decided to pellet the EVs using a TCA precipitation protocol. Following several attempts to perform this protocol, the final protocol was kindly provided by Prof/Dr. Giricz Zoltan, Hungary (Baranyai et al., 2015).

3.1. The EVs isolated by ultracentrifugation, ExoQuick kit and by qEV SEC columns (unpooled fractions) presented different size ranges

EVs were isolated from the plasma of MM patients by ultracentrifugation, ExoQuick and by qEV SEC columns. In order to confirm if it was possible to detect (or preferably to isolate) different populations of EVs in each of the isolates, each of the obtained EVs were analyzed for size distribution using DLS. Interestingly, the three protocols tested consistently provided EVs with different sizes (**Figure 5, Tables 1, 2 and 3**). The ultracentrifugation method allowed to isolate mainly larger vesicles, with a diameter between 100 to 1000 nm, which is associated to the size of microvesicles. The ExoQuick kit isolated smaller vesicles, with a size ranging from 10 to 100 nm, associated to the size of exosomes. Interestingly, the qEV SEC columns allowed the isolation of at least two different populations of EVs. In particular, the first three collected fractions (fractions 7 to 9) presented EVs with a size range between 100 to 1000 nm, which was completely different from the size range between 10 to 100 nm of the EVs eluted in later fractions (fractions10 to 12). These results are in accordance with what was expected, since the larger vesicles elute more rapidly than the smaller ones, which were collected at latter fractions (**Figure 5**).

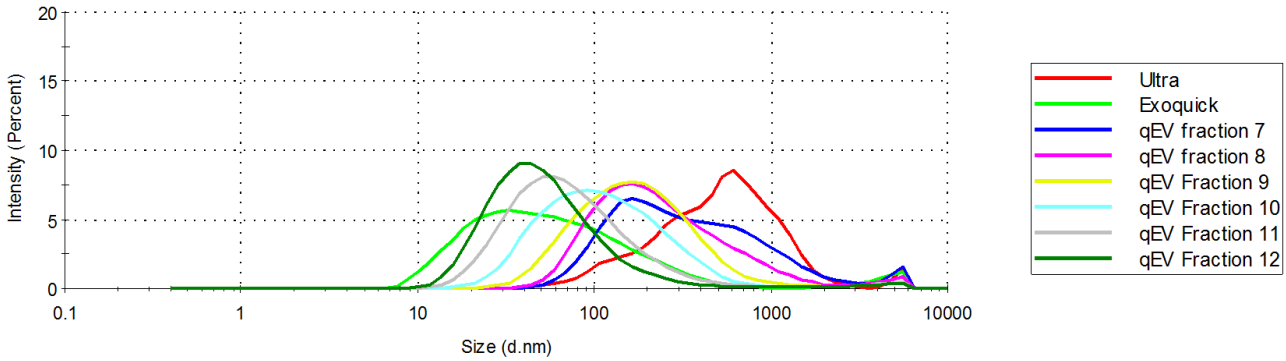

Figure 5 – Size distribution obtained from dynamic light scattering (DLS) analysis of EVs isolated by ultracentrifugation, with the ExoQuick kit or by qEV size exclusion chromatography columns (SEC; various fraction collected from the columns are shown – fractions 7 to 12). MM plasma EVs were isolated by three different methods. The ultracentrifugation protocol isolated mainly particles ranging in size from 100 to 1000 nm. The ExoQuick kit predominantly isolated vesicles in the range of exosomal size-like particles, between 30 to 100 nm. The typical size of EVs obtained by qEV SEC columns was found to be between 100 to 1000 nm for the early collected fraction (7, 8 and 9), while vesicles isolated at latter fractions (10,11 and 12) ranged from 30 to 100 nm in diameter. Results represent the mean of at least 6 independent experiments; ultracentrifugation n=7, ExoQuick kit n=6, qEV SEC columns n=8. Size distribution was measured with the Zetasizer Nano ZS and the results were generated by the Zetasizer software version v7.11.

EVs were further analysed by TEM. The main objective of this analysis was to confirm the presence of EVs in the isolates and to evaluate how pure the EVs were, by searching for the presence of contaminants or proteins aggregates.

However, the images obtained from the ultracentrifugation isolates showed a majority of particles with a perfect round shape, which is not characteristic of vesicles-like particles. These particles, with a size range from 25 to 200 nm (for patient 18) or to 500 nm (for patient 34) did not present either a cup shape or a perceptible lipid bilayer, suggesting the isolation of lipoproteins (white spheres). In addition, in some images, it was possible to see protein aggregates and structures with a damaged membrane (**Figure 6A**).

The images of the vesicles obtained with the ExoQuick kit showed a high amount of vesicles (in both of the patient's samples analysed), which made the analysis more difficult. However, it was possible to verify that both isolates were very homogeneous and contained vesicles with a size ranging from approximately 30 nm to 100 nm. Protein aggregates and other contaminants were also evident (**Figure 6B**).

In case of EVs obtained with the qEV SEC protocol, a third objective was to confirm the data obtained by DLS and to recognize the fractions that contained the populations of EVs with sizes above 100 nm (typical of microvesicles) and the ones with smaller size, below 100 nm (typical of exosomes). That information would allow latter to pool the fractions that had similar EVs. However, the first fractions (fractions 7 to 9, which from the DLS data seemed to contain microvesicles) presented perfectly round shaped particles, suggesting the presence of lipoproteins rather than microvesicles. In later fractions, smaller EVs were noticed; however, the number of protein aggregates also increased in fractions 10 to 12. Additionally, in some cases it was not possible to conclude if the particles observed were structures from the columns that co-eluted with vesicles or contaminants (**Figure 6C**).

3.2. The EVs isolated by ultracentrifugation, ExoQuick kit and by qEV SEC columns present markers of EVs

Having studied the size of EVs isolated with the different methods, the analysis of EVs markers for each of the isolates obtained with the three protocols was carried out. In particular, the tetraspanins family proteins (CD63, CD9 and CD81) and cytosolic proteins (Hsp70 and syntenin-1) were analysed. Other proteins were also studied: cytoskeletal proteins (actin and tubulin – in order to see if it was possible to use them as "loading control"), cell organelle markers (cytochrome c – in order to confirm that there were no cell contaminants), and a plasma protein (albumin – to study the possible presence of protein contaminants from plasma).

The detection of EVs markers by Western blot was a challenging task, since some methods displayed lower amounts of protein obtained from the EV lysates. In particular, ultracentrifugation and the three first fractions (fraction 7, 8 and 9) obtained from the qEV SEC columns allowed to obtain less than 5µg of protein. Therefore, different amounts of proteins were loaded into the Western blot gels.

Actin and tubulin proved not to be good loading controls for EVs. This is probably the reason why, some authors have not been included any loading control for proteins isolated from EVs in their studies (Baranyai et al., 2015; Cheng et al., 2014; Hong et al., 2016; Lobb et al., 2015; Van Deun et al., 2014). In other studies, the Ponceau staining of

the EVs lysates were presented, to show that different amounts of protein were loaded in each lane (**Figure 7B**), as often done in the EVs literature (Harshman et al., 2016).

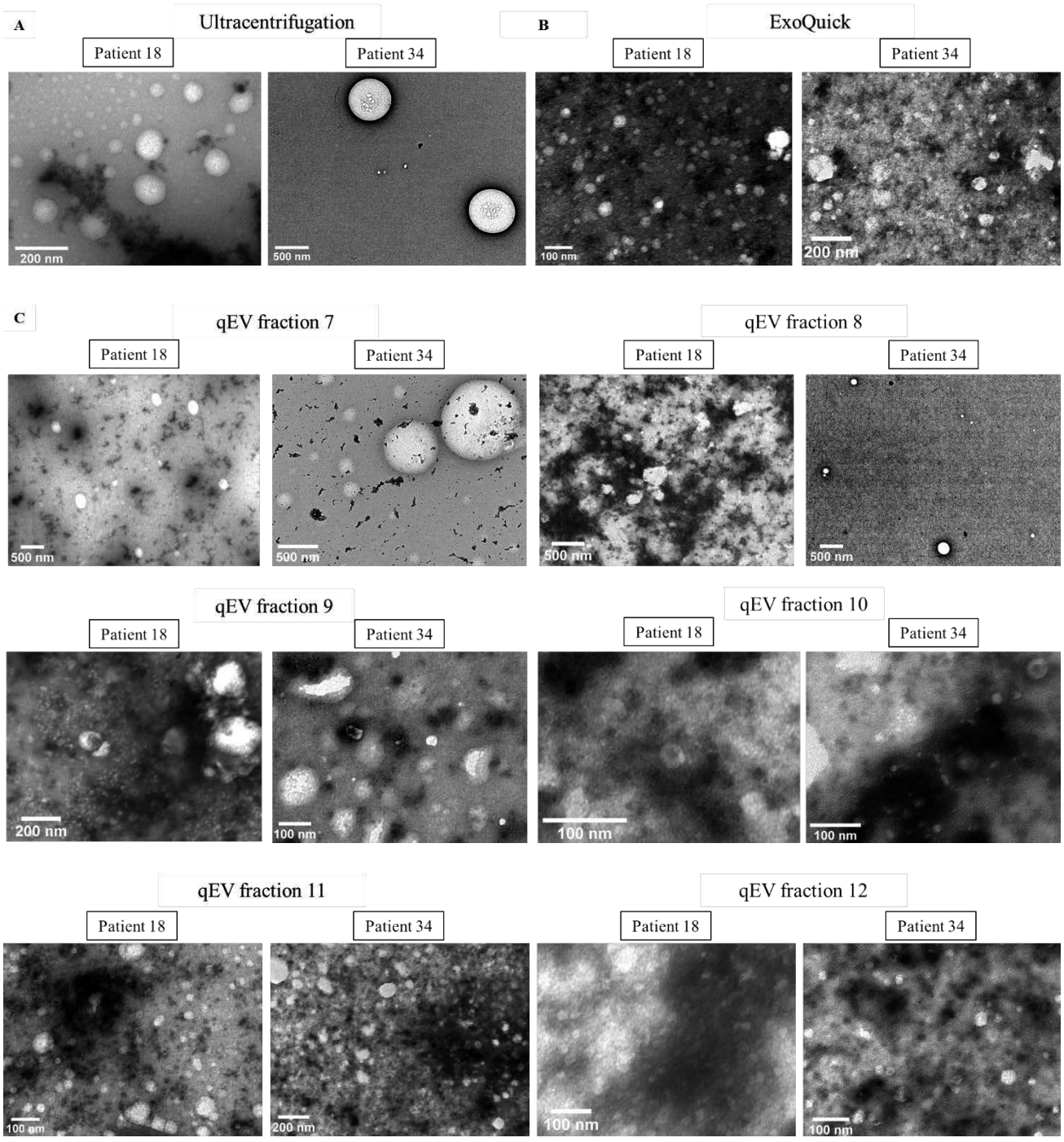

Figure 6 –Transmission electron microscopy (TEM) images of EVs isolated from plasma of two MM patients by (A) ultracentrifugation, (B) ExoQuick and (C) qEV SEC columns. Isolates obtained by ultracentrifugation, ExoQuick kit or eluted from different fractions of the qEV SEC columns were analyzed by TEM for the presence of vesicles. Additionally, TEM allowed to morphologically characterize EVs after being submitted to each protocol and to assess the purity of isolates based on the occurrence of protein aggregates and lipoprotein-like particles. Scale bar is 100 nm, 200 nm or 500 nm.

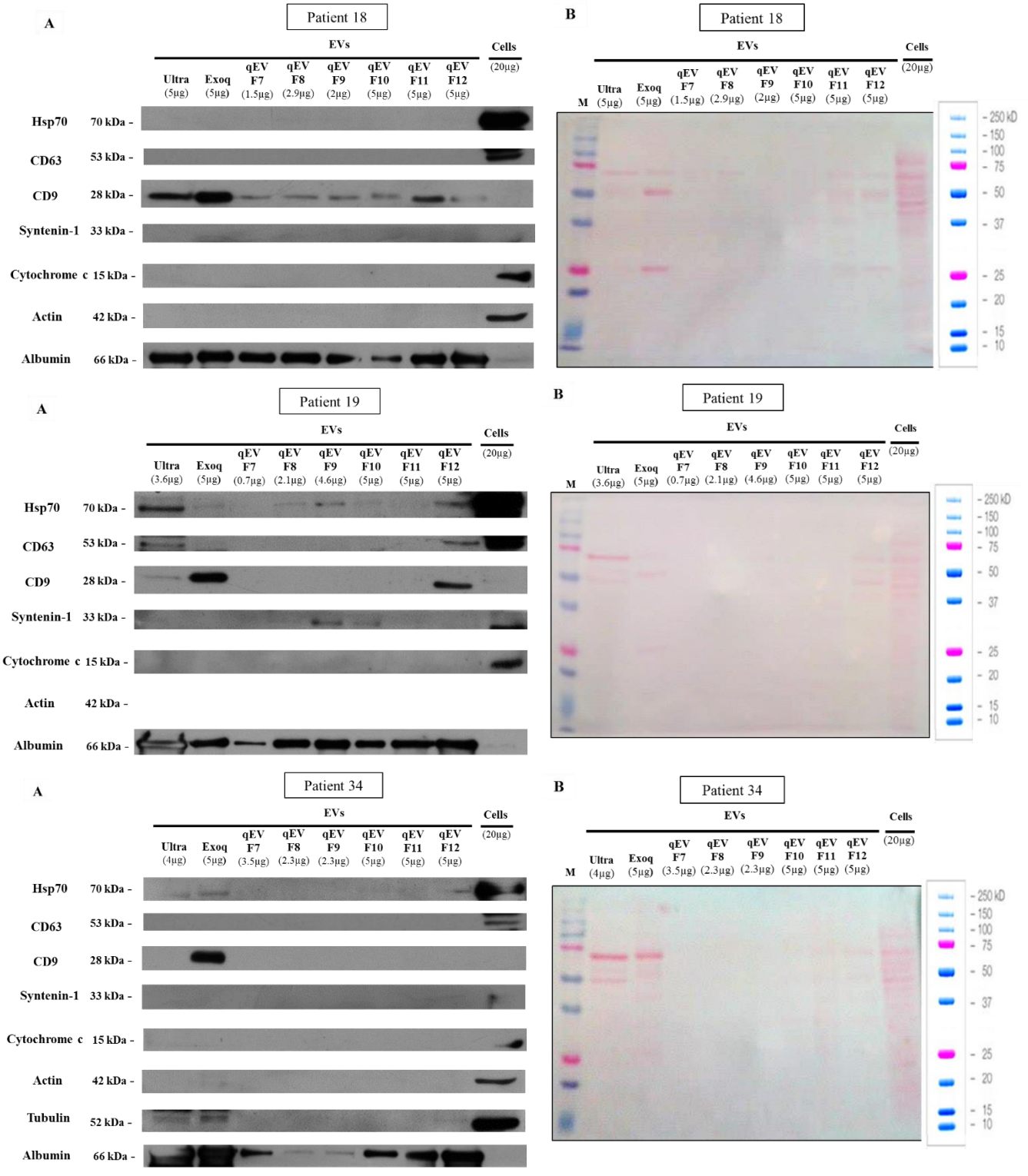

Figure 7 – Analysis of protein markers of EVs by Western blot analysis of the lysates of EVs isolated by different methods (A) and corresponding Ponceau protein staining for confirmation of loading (B). Plasma EVs isolated from three MM patients (patient 18, patient 19 and patient 34) by three different methods: ultracentrifugation, ExoQuick and qEV SEC columns. The amount of protein loaded depended on the quantity available. Vesicles isolated by ultracentrifugation (2-5 µg of protein loaded into the gel), Exoquick kit (5 µg of protein) and from qEV SEC size exclusion columns collected in 0,5 ml fractions (~0,7-5 µg of protein obtained per

fraction) were analyzed by Western blot. RPMI-8226 MM cells lysate were used as control (20 µg of total protein loaded). Proteins analysed were: EVs positive markers (Hsp70, CD63, CD9, Syntenin-1), cell organelle markers (cytochrome c), structural proteins (actin and tubulin) and the abundance of a plasma protein (albumin). Ponceau staining of the EVs lysates shows that different amounts of protein were loaded in each lane.

The blots showed the presence of EVs markers in the samples obtained with the three different methods (**Figure 7A**). However, inconsistent results were obtained for the three patients analysed. The CD9 (28 kDa) marker was clearly detected at higher levels in the EVs isolated with the ExoQuick kit, in the plasma samples of all of the three patients. In case of EVs isolated by ultracentrifugation and the in last collected fraction of the qEV SEC columns (fraction 12), CD9 detection was also possible but at lower levels and only in two patients, while the CD63 (53 kDa) and Hsp70 (70 kDa) markers were found in isolates from only one patient. Hsp70 expression was also found at the fractions 8 to 10 for patient 19.

For patient 18, weaker bands of the CD9 marker were also found in fractions from 7 to 11 from the qEV SEC columns, refuting the hypothesis that CD9 expression could be found only at the exosomal-like vesicles isolated with the ExoQuick kit (previously shown to isolate mainly smaller particles, with a size range from 10 to 100nm). Surprisingly, syntenin-1 (33 kDa) was only detected in fractions 9 and 10 collected (from the qEV SEC columns) from the plasma of patient number 19, which could be hypothesized as a marker for the presence of microvesicles (since it was assumed that fractions 9 and 10 of the qEV SEC columns isolated larger EVs). However, the results obtained with syntenin-1 for patient 19 were not reproduced in the samples from the other two patients analysed (**Tables 1**, **2** and **3**).

The cytochrome c results indicate that all the methods isolated EVs without cellular contaminants. Additionally, the albumin signal was very strong (bands around 66 kDa) for the three protocols, corroborating the results obtained with the TEM images and proving that all methods isolate protein contaminants (from plasma) together with the EVs.

In summary, all the three methods isolated vesicles presenting EV markers, with no apparent cellular contaminants but with protein contaminants.

Table 1. Summary of the results obtained for the characterization of the EVs isolated by ultracentrifugation

Ultracentrifugation *Samples*	*EVs Patient 18*	*EVs Patient 19*	*EVs Patient 34*
Size in nm *(% intensity)*	466.7 nm (95.1%)	334.3 nm (94.0%)	315.7 nm (94.1%)
	115.5 nm (4.9%)	5058 nm (3.8%)	5225 nm (5.1%)
	0.0	53.96 nm (2.2%)	73.78 nm (0.8%)
Average size in mm	543.3 nm	312.6 nm	422.3 nm
Protein concentration in µg/ml *(µg of total protein in total volume)*	779.0 µg/ml (15.6 µg in 20 µl)	164.7 µg/ml (3.6 µg in 22 µl)	173.7 µg/ml (4 µg in 23 µl)
Presence of EVs markers/cell organelle markers/albumin	CD9 + Albumin ++	Hsp70 CD63 CD9 Albumin ++	Hsp70 Tubulin Albumin +++
Presence of Protein aggregates/ Lipoproteins	Protein aggregates ++ Lipoproteins ++	n.d.*	Protein aggregates + Lipoproteins ++
RNA concentration in ng/µl *(ng of total RNA in total volume)*	RNAse treatment 4.6 ng/µl (230 ng in 50 µl)	7.3 ng/µl (365 ng in 50 µl)	RNAse treatment 6.4 ng/µl (320 ng in 50 µl)

* n.d. = not determined

Table 2. Summary of the results obtained for the characterization of the EVs isolated with the ExoQuick kit

ExoQuick *Samples*	*EVs Patient 18*	*EVs Patient 19*	*EVs Patient 34*
Size in nm *(% intensity)*	97.6 nm (53.3%) 17.8 nm (41.6%) 2946 nm (5.1%)	53.2 nm (97.0%) 4498 nm (3 %) 0.0	101.6 nm (98.8%) 3541 nm (1.2%) 0.0
Average size in mm	31.8 nm	41.9 nm	59.7 nm
Protein concentration in µg/ml *(µg of total protein in total volume)*	1555.3 µg/ml (1283.1 µg in 825 µl)	1947.8 µg/ml (1071.3 µg in 550 µl)	2200.1 µg/ml (110.0 µg in 50 µl)
Presence of EVs markers/cell organelle markers/albumin	CD9 ++ Albumin ++	Hsp70 CD9 Albumin ++	Hsp70 CD9 ++ Tubulin Albumin ++
Presence of Protein aggregates/lipoproteins	Protein aggregates +	n.d.*	Protein aggregates +
RNA concentration in ng/µl *(ng of total RNA in total volume)*	RNAse treatment 6,9 ng/µl (345 ng in 50 µl)	4,0 ng/µl (200 ng in 50 µl)	RNAse treatment 4,7 ng/µl (235 ng in 50 µl)

* n.d. = not determined

Table 3. Summary of the results obtained for the characterization of the EVs isolated with the qEV SEC columns: analysis of fractions 7 to 12

qEV columns	*EVs Patient 18*						*EVs Patient 19*						*EVs Patient 34*					
Samples	*F7*	*F8*	*F9*	*F10*	*F11*	*F12*	*F7*	*F8*	*F9*	*F10*	*F11*	*F12*	*F7*	*F8*	*F9*	*F10*	*F11*	*F12*
Size in nm *(% intensity)*	231.2 nm (94.7%)	209.4 nm (98.7%)	176.6 nm (99.9%)	130.1 nm (98.5%)	66.17 nm (97.8%)	45.25 nm (96.9%)	562.5 nm (59.8%)	383.0 nm (97.4%)	122.1 nm (81.7%)	139.1 nm (98.5%)	68.98 nm (97.1%)	57.58 nm (99.5%)	175.1 nm (100%)	161.9 nm (100%)	137.7 nm (100%)	85.57 nm (99.4%)	66.98 nm (98.6%)	57.91 nm (99.5%)
	4466 nm (5.3%)	4184 nm (1.3%)	16.55 nm (0.1%)	3495 nm (1.5%)	4194 nm (2.2%)	3385 nm (3.1%)	128.9 nm (37.5%)	4657 nm (2.6%)	1179 nm (18.3%)	3831 nm (1.5%)	4276 nm (2.9%)	4623 nm (0.5%)	0.0	0.0	0.0	4303 nm (0.6%)	4557 nm (0.9%)	4590 nm (0.5%)
	0.0	0.0	0.0	0.0	0.0	0.0	5217 nm (2.8%)	0.0	0.0	0.0	0.0	0.0	0.0	0.0	0.0	0.0	1089 nm (0.4%)	0.0
Average size in nm	193.8 nm	158.4 nm	124.1 nm	72.62 nm	46.61 nm	36.09 nm	251.9 nm	156.3 nm	111.4 nm	79.28 nm	59.74 nm	48.14 nm	143.3 nm	132.6 nm	105.7 nm	70.83 nm	55.44 nm	46.82 nm
Protein concentration in µg/ml *(µg of total protein in total volume)*	102.9 µg/ml (1.5 µg in 15 µl)	191.2 µg/ml (2.9 µg in 15 µl)	101.4 µg/ml (2.0 µg in 20 µl)	430.3 µg/ml (17.2 µg in 40 µl)	1351.4 µg/ml (67.6 µg in 50 µl)	2627.7 µg/ml (131.4 µg in 50 µl)	33.7 µg/ml (0.7 µg in 20 µl)	104.5 µg/ml (2.1 µg in 20 µl)	230.5 µg/ml (4.6 µg in 20 µl)	388.0 µg/ml (15.5 µg in 40 µl)	332.9 µg/ml (13.3 µg in 40 µl)	1781.7 µg/ml (89.1 µg in 50 µl)	173.7 µg/ml (3.5 µg in 20 µl)	114.7 µg/ml (2.3 µg in 20 µl)	114.7 µg/ml (2.3 µg in 20 µl)	686.9 µg/ml (27.5 µg in 40 µl)	555.3 µg/ml (22.2 µg in 40 µl)	844.8 µg/ml (50.7 µg in 60 µl)
Presence of EVs markers/cell organelle markers/albumin	CD9 Albumin ++	CD9 Albumin ++	CD9 Albumin ++	CD9 Albumin +	Hsp70 CD9 + Albumin ++	Hsp70 CD9 + Albumin ++	Albumin +	Syntenin-1 Albumin ++	Syntenin-1 Albumin ++	Syntenin-1 Albumin ++	Albumin ++	CD63 CD9 + Albumin ++	Albumin +	Albumin	Albumin	Albumin +	Albumin ++	Tubulin Albumin ++
Presence of Protein aggregates/ Lipoprotein	Protein aggregates Lipoprotein ++	Protein aggregates Lipoprotein +	Protein aggregates	Protein aggregates +	Protein aggregates +	Protein aggregates +	n.d.*	n.d.*	n.d.*	n.d.*	n.d.*	n.d.*	Protein aggregates Lipoprotein ++	Protein aggregates Lipoprotein ++	Protein aggregates	Protein aggregates +	Protein aggregates +	Protein aggregates ++
RNA concentration in ng/µl *(ng of total RNA in total volume)*	RNase treatment 5.4 ng/µl (270 ng in 50 µl)						5.6 ng/µl (280 ng in 50 µl)						RNase treatment 8.8 ng/µl (440 ng in 50 µl)					

* n.d. = not determined

3.3. The EVs isolated by ultracentrifugation, ExoQuick kit and by the pooled fractions of the qEV SEC columns also presented different size ranges and EV markers

Since the previous study with unpooled fractions from the qEV SEC columns allowed to isolate small amounts of proteins in most of the fractions, an analysis of the pooled fractions was also carried out (for patients 20, 21 and patient 22) and compared with the other two methods.

DLS analysis of the ultracentrifugation protocol (**Figure 8A**) and ExoQuick kit (**Figure 8B**) showed similar results to the ones previously shown in **Figure 5**. The size distribution of the pooled EVs isolated with the qEV SEC columns showed distinct populations of EVs, that might correspond to exosomes (around 40 nm and 150 nm) and microvesicles (the latter peak) (**Tables 4, 5** and **6**).

DLS measures the light scattered by particles, and thus it does not distinguish particles from contaminants. It was noticed that the three methods showed a peak around 5 000 nm, that probably results from contaminating particles or aggregates. TEM analysis was not performed for these tested patients, however the Western blot analysis for plasma contaminants, such as albumin, could give additional information about the purity of isolates (please see below).

Overall, the ultracentrifugation and the qEV SEC columns (**Figure 8C**) allowed the isolation of heterogeneous populations, while the ExoQuick apparently only isolated exosomal-like particles. Since the main goal is to find the best suited protocol to study all the EVs released from MM plasma cells, the ExoQuick kit was found an unsuitable method for that purpose.

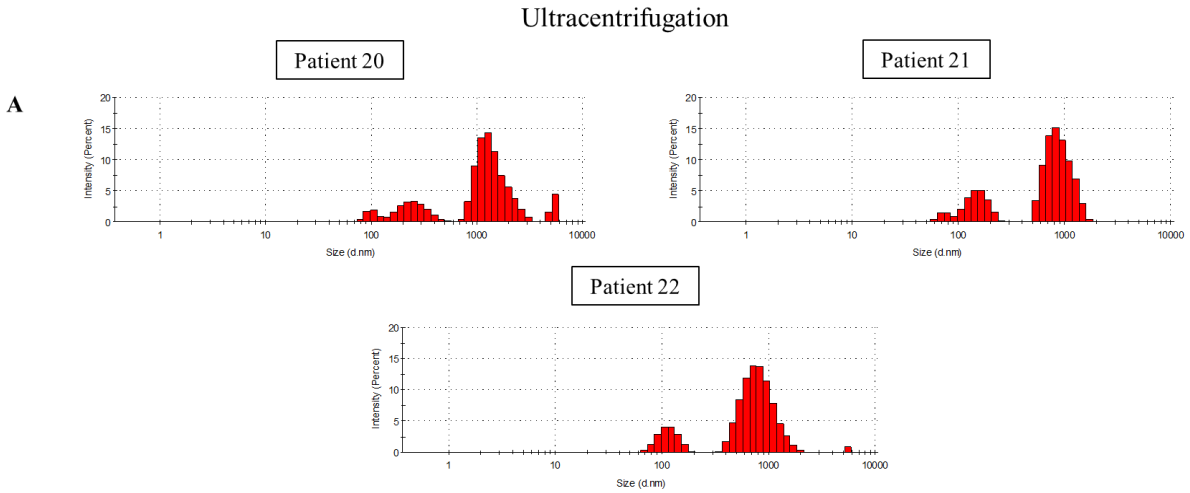

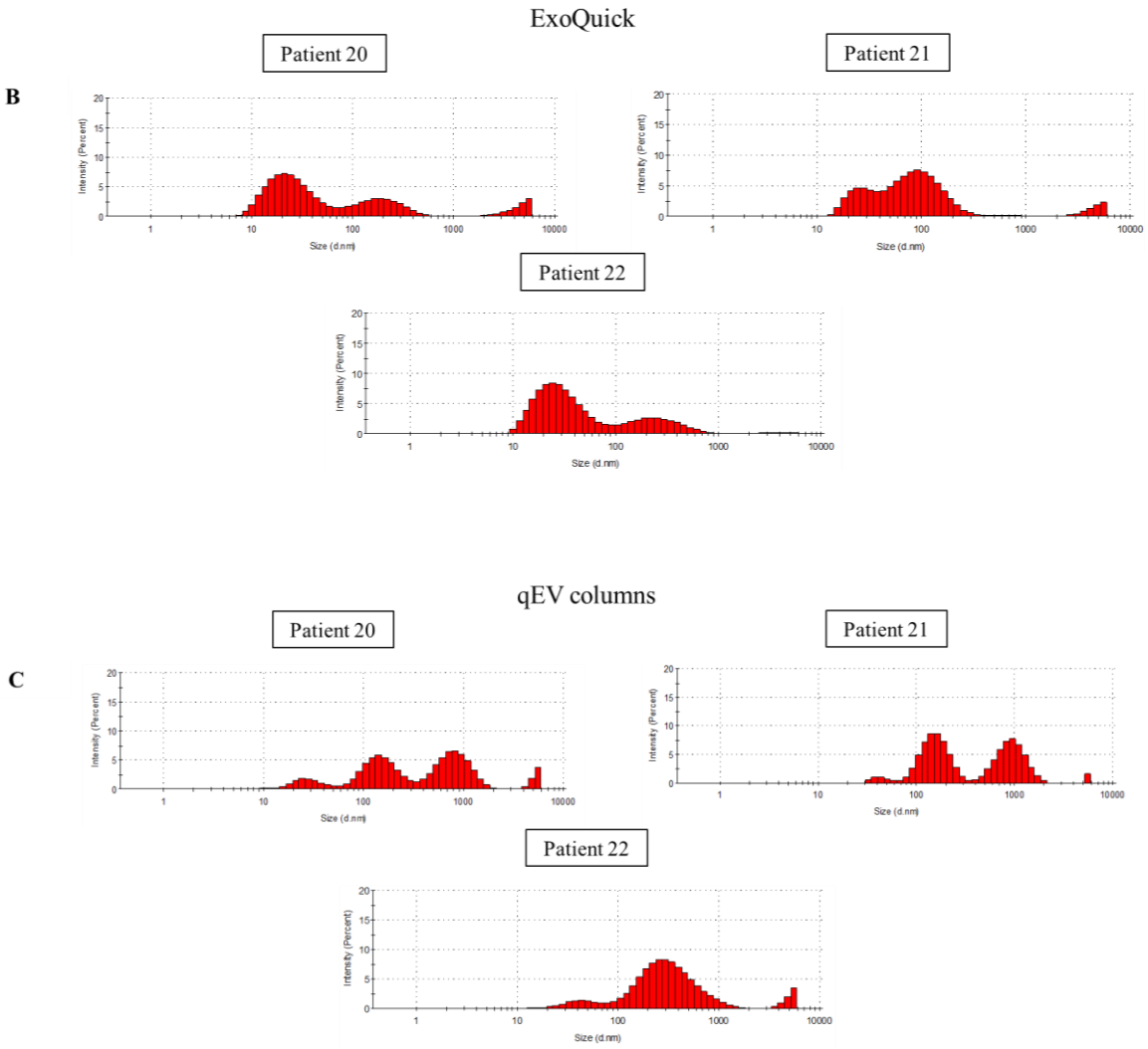

Figure 8 – Size distribution obtained from dynamic light scattering (DLS) analysis of EVs isolated by (A) ultracentrifugation, with the (B) Exoquick kit or by (C) qEV size exclusion chromatography columns (SEC; with a pool of fractions 7 to 12). Plasma EVs isolated from three MM patients (patient 20, patient 21 and patient 22) by three different methods. The typical size of EVs isolated with the ExoQuick kit was in the size range of 30-100 nm; while the isolates obtained by ultracentrifugation or with the SEC protocols showed not only exosomal-like particles, but also vesicles with a size range typical of microvesicles (100-1000nm). Results are the average of three measurements obtained with the Zetasizer Nano ZS and generated by the Zetasizer software version v7.11.

After the size characterization, the expression of specific EVs markers was analysed, as for the previous experiments (please see above, Section 3.1) The EV markers analysed were CD63, CD9, CD81, Hsp70, Syntenin-1, CHMP4B and ARF6. The cytoskeletal proteins actin and tubulin were also analysed, in order to see if they could be used as loading controls; cytochrome c was analysed to verify if there was cell contaminants; and the plasma protein albumin was also analysed to confirm if there were protein contaminants from plasma.

By pooling the fractions from the qEV SEC columns, higher amounts of protein were obtained for the Western blot analysis. The protein levels recovered with the ultracentrifugation protocol were almost identical from the previously obtained (5 µg); similarly, the ExoQuick kit provided higher amounts of protein level as previously obtained. The differences in the amounts of total proteins isolated with the different protocols (with pooled and unpooled fractions in the qEV SEC columns) are shown in **Figure 9**.

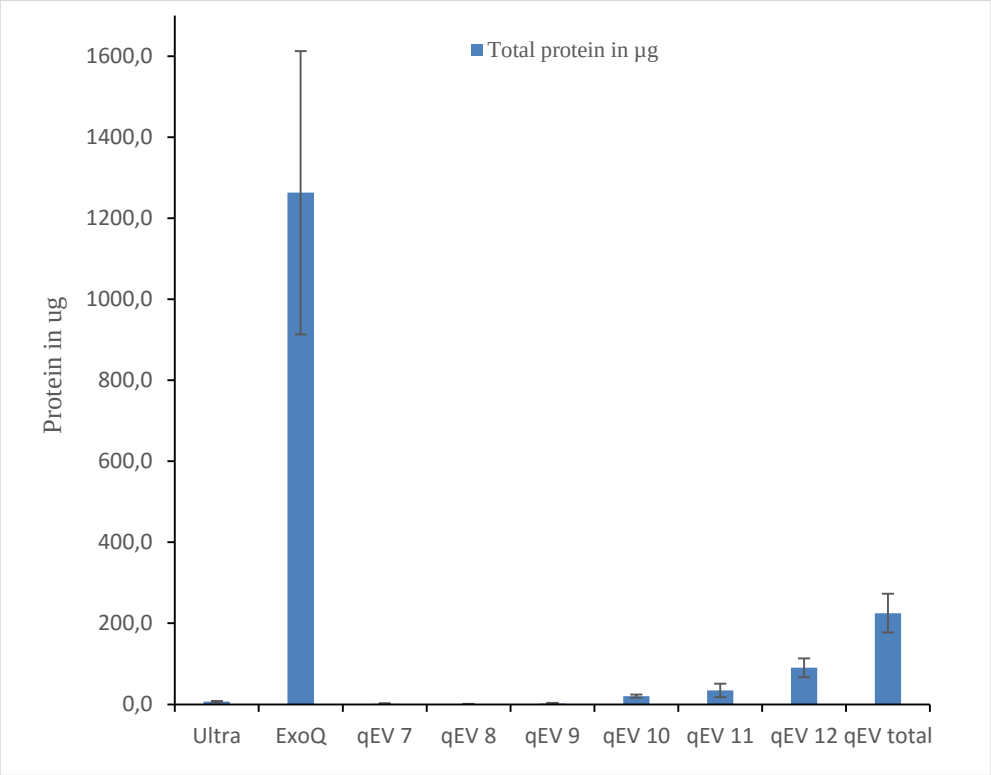

Figure 9 – Total protein yields recovered from the EV pellets obtained by ultracentrifugation, ExoQuick kit and fractions 7 to 12 of the qEV SEC columns or from pooled fractions from the same qEV SEC columns. Protein quantification was determined with modified Lowry assay (Bio-Rad). Total amount of protein quantified in µg (micrograms). Results are the mean of at least 3 independent biological replicates (Ultracentrifugation n=7, ExoQuick kit n=6, qEV SEC fractions 7 to 12 n=3, and pooled fractions from qEV SEC n=3).

The amount of protein recovered with the ExoQuick kit was repeatedly higher when compared with the protein levels obtained either with the ultracentrifugation or with the qEV SEC columns. The differences in the protein levels are even more evident when comparing ExoQuick with single fractions collected from the columns (**Figure 9**). The results obtained with the ExoQuick were surprising, since it required the lowest amount of starting sample (250 µl of plasma). However, this higher amount of proteins may have a non-exosomal origin, since polymer-based precipitation appears to highly precipitate circulating proteins (Taylor & Shah, 2015). The ultracentrifugation allowed the precipitation of lower amounts of protein compared to the other two methods **(Figure 9)**, even though this protocol required large amounts of starting samples (about 1000 µl to 1250 µl of plasma). This could be explained by the fact that, at high speeds and with increased duration of the ultracentrifugation steps, the EVs membrane may be damaged (Baranyai et al., 2015). The qEV SEC columns with pooled fractions allowed the recovery of enough total protein from the EVs, suitable for analyses by Western blot. However, as previously mentioned **(section 3.2)** the unpooled fractions had not provide enough quantity of total proteins to be properly analysed by Western Blot. The qEV SEC protocol may be performed with approximately 500 µl to 1000 µl of starting sample (plasma).

Therefore, it was possible to load 20 µg of protein for the EVs isolated with the ExoQuick kit and the qEV SEC columns; nonetheless, lower amounts of protein were loaded for the EV lysates obtained by ultracentrifugation (in which the protein loaded depended on the quantity available).

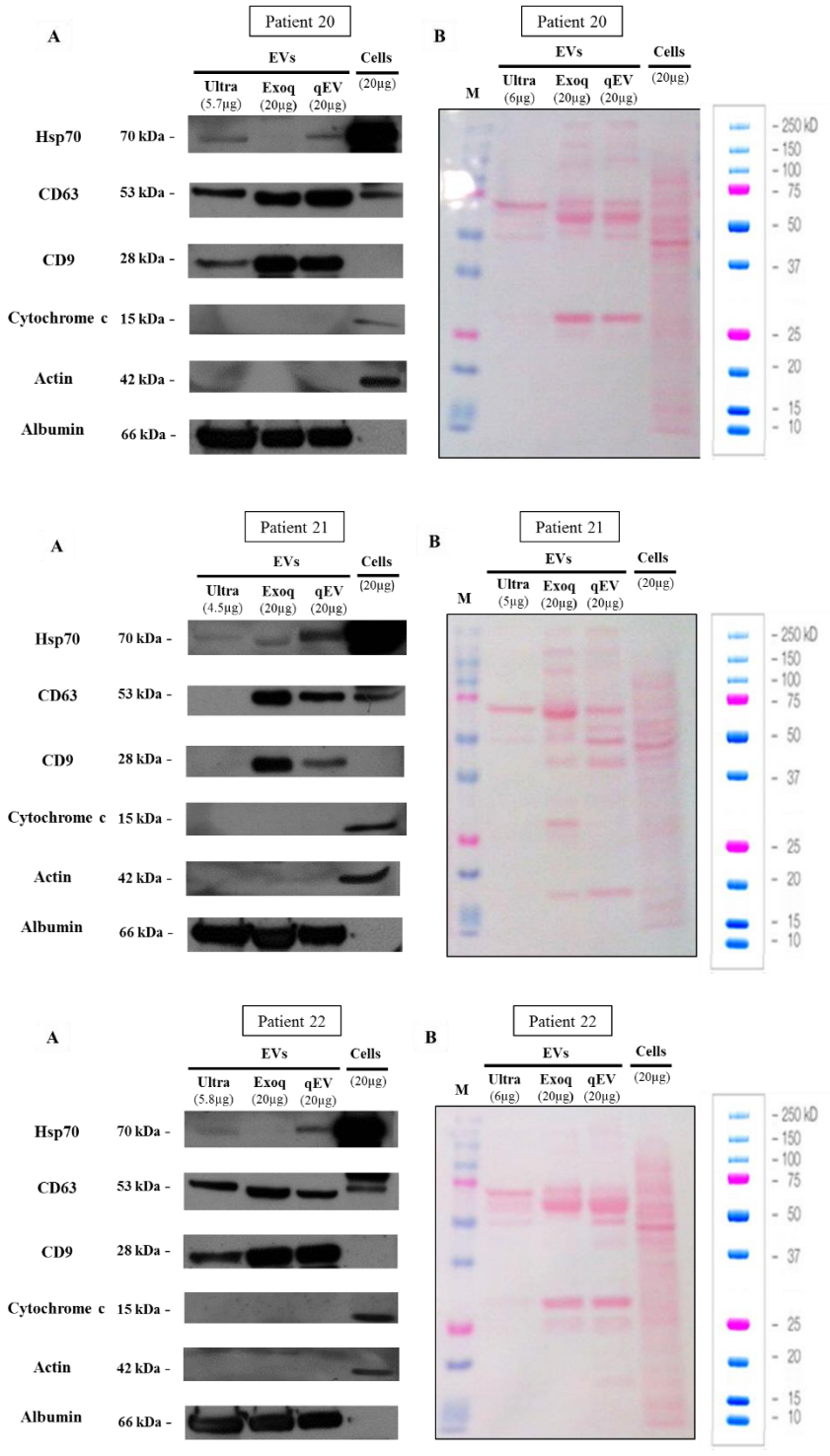

Figure 10 – Analysis of protein markers of EVs by Western blot analysis of the lysates of EVs isolated by different methods (A) and corresponding Ponceau protein staining for confirmation of loading (B). EVs were obtained from MM plasma samples derived from three different patients (patient 20, patient 21 and patient 22). RPMI-8226 MM cell lysate was used as control (20 µg of total protein loaded). The amount of EV protein loaded depended on the quantity available. EVs were isolated by ultracentrifugation (5-6 µg of protein obtained and loaded into the gel), Exoquick kit (20 µg of protein loaded into the gel) and qEV SEC columns (20 µg of protein loaded into the gel). Proteins analysed were: EV positive markers (Hsp70, CD63 and CD9), cell organelle markers (cytochrome c and actin) and the most abundant protein in plasma (albumin), in RPMI-8226 MM cells and EVs. The Ponceau staining of the EV lysates loaded into

the gel shows that different amounts of protein were loaded in each lane (5 or 6 µg loaded for Evs isolated by the ultracentrifugation method, 20 µg loaded for EVs isolated by the other two methods).

In the EVs obtained by ultracentrifugation, weaker bands were obtained for all the markers, since lower amounts of total protein were loaded into the gel.

The EVs isolated from the three patients (patient 20, 21 and 22) with the ultracentrifugation and the qEV SEC columns presented Hsp70, while with the ExoQuick kit, Hsp70 was barely detected in one patient. This may suggest that EVs isolated with the ExoQuick kit are poorer in the Hsp70 marker. In contrast, the EVs isolated with the ExoQuick kit were highly enriched in CD63 and CD9. These results, together with the previously mentioned size characterization, suggest a tendency for higher expression of CD63 and CD9 in exosomal isolates (rather than in larger EVs). Indeed, this association of CD63 and CD9 expression markers with exosomes has been previously demonstrated (Kowal et al., 2016).

Additional EV markers were also tested, such as syntenin-1, CHMP4 and ARF6, but they were not detected in any of the EVs tested (data not shown). Indeed, not all of the EVs markers are always present (or found by Western Blot) in all of the EVs (Yoshioka et al., 2013).

The qEV SEC columns were the method that allowed the detection of more EVs markers and provided more reproducible results for the three patients. However and unfortunately, it was not possible to obtain EV preparations free of contaminants when using the qEV SEC columns, which had been previously described by other authors as being an effective method to isolate highly pure EVs when compared to the ultracentrifugation or the ExoQuick kit (Lobb et al., 2015). Alternatively to the used method, the same authors have included a further filtering step, prior to the chromatography, to concentrate the EVs and simultaneously to remove additional contaminating proteins. However, they have also described the presence of albumin in their isolates (Lobb et al., 2015). Therefore, future work should include further sample treatments, such as a centrifugation at low-speed or a filtration step, prior to loading the samples into the columns (Szatanek et al., 2015). Thus, the use of qEV SEC columns may be further optimized, for the recovery of more pure EVs.

In general, the Western blot results supported the presence of EVs in the isolates obtained from the different methodologies studied. Furthermore, it confirmed the presence of contaminating albumin in all the isolates.

Table 4. Summary of the results obtained for the characterization of the EVs isolated by ultracentrifugation

Ultracentrifugation *Samples*	***EVs*** ***Patient 20***	***EVs*** ***Patient 21***	***EVs*** ***Patient 22***
Size in nm *(% intensity)*	1431 nm (70.8%) 258.7 nm (17.8%) 5360 nm (5.9%)	1010 nm (88.9%) 151.7 nm (4.8%) 75.88 nm (6.2%)	822.1 nm (82.2%) 115.9 nm (16.9%) 5560 nm (0.9%)
Average size in mm	1017 nm	905.2 nm	640.2 nm
Protein concentration in µg/ml *(µg of total protein in total volume)*	229.1 µg/ml (5.7 µg in 25 µl)	180.2 µg/ml (4.5 µg in 25 µl)	242.3 µg/ml (5.8 µg in 24 µl)
Presence of EVs markers/cell organelle markers/albumin	Hsp70 CD63 + CD9 + Albumin +++	Hsp70 Albumin +++	Hsp70 CD63 + CD9 + Albumin +++
RNA concentration in ng/µl *(ng of total RNA in total volume)*	7.7 ng/µl (385 ng in 50 µl)	6.0 ng/µl (300 ng in 50 µl)	6.8 ng/µl (340 ng in 50 µl)

Table 5. Summary of the results obtained for the characterization of the EVs isolated with the ExoQuick kit

ExoQuick *Samples*	***EVs*** ***Patient 20***	***EVs*** ***Patient 21***	***EVs*** ***Patient 22***
Size in nm *(% intensity)*	25.9 nm (62.5%) 194.8 nm (28.4%) 4473 nm (9%)	103.7 nm (67.6%) 26.7 nm (25.0%) 4577 nm (6.6%)	31.3 nm (72.6%) 266.8 nm (26.4%) 3867 nm (1%)
Average size in mm	42.5 nm	62.4 nm	33,5 nm
Protein concentration in µg/ml *(µg of total protein in total volume)*	1976.1 µg/ml (1976.1 µg in 1000 µl)	671.2 µg/ml (671.2 µg in 1000 µl)	2465.5 µg/ml (2465.5 µg in 1000 µl)
Presence of EVs markers/cell organelle markers/albumin	CD63 ++ CD9 ++ Albumin ++	Hsp70 CD63 ++ CD9 ++ Albumin +++	CD63 + CD9 ++ Albumin ++
RNA concentration in ng/µl *(ng of total RNA in total volume*	5.0 ng/µl (250 ng in 50 µl)	5.4 ng/µl (270 ng in 50 µl)	5.6 ng/µl (280 ng in 50 µl)

Table 6. Summary of the results obtained for the characterization of the EVs isolated with the SEC columns: analysis of pooled fractions 7 to 12

qEV columns *Samples*	***EVs Patient 20*** ***Pooled fractions***	***EVs Patient 21*** ***Pooled fractions***	***EVs Patient 22*** ***Pooled fractions***
Size in nm *(% intensity)*	825.5 nm (44.2%) 159.2 nm (39.0%) 30.0 nm (11%)	161.5 nm (49.0%) 947.9 nm (45.3%) 45.7 nm (4.1%)	362.2 nm (83.9%) 45.0 nm (9.6%) 5045 nm
Average size in mm	232.9 nm	405.3 nm	257.8 nm
Protein concentration in µg/ml *(µg of total protein in total volume)*	2180.5 µg/ml (218.1 µg in 100 µl)	1463.6 µg/ml (146.4 µg in 100 µl)	3111 µg/ml (311.1 µg in 100 µl)
Presence of EVs markers/cell organelle markers/albumin	Hsp70 CD63 ++ CD9 ++ Albumin ++	Hsp70 CD63 + CD9 Albumin ++	Hsp70 CD63 + CD9 ++ Albumin ++
RNA concentration in ng/µl *(ng of total RNA in total volume)*	4.1 ng/µl (205 ng in 50 µl)	5.3 ng/µl (265 ng in 50 µl)	5.2 ng/µl (260 ng in 50 µl)

3.4. Preliminary results indicate that the EVs isolated by ultracentrifugation, ExoQuick kit and by qEV SEC columns apparently have different amounts of miR-21 and miR-16

The analysis of miRs was then carried out in the EVs isolated with the different methods. Since extracellular miRs not only circulate inside of the EVs but also in protein complexes (Arroyo et al., 2011; El-Hefnawy et al., 2004; Turchinovich et al., 2011), it was decided to attempt a comparison of the levels of miRs isolated with the different methods, in samples treated and untreated with RNase. Therefore, the EVs from two patient samples were pre-treated with RNAse enzyme.

The RNA extraction protocol was then equally performed, for the samples treated or untreated with RNAse. The total amount of RNA isolated was very similar for the different EV isolation methods **(Figure 11)**. Indeed, in a total of six samples analysed (from 6 different patients), the RNA concentrations obtained from EVs isolated by the ultracentrifugation protocol were from 4.6 to 7.7 ng/µl, for the ExoQuick kit were from 4 to 6.9 ng/µl and for the qEV SEC columns between 4.1 and 8.8 ng/µl.

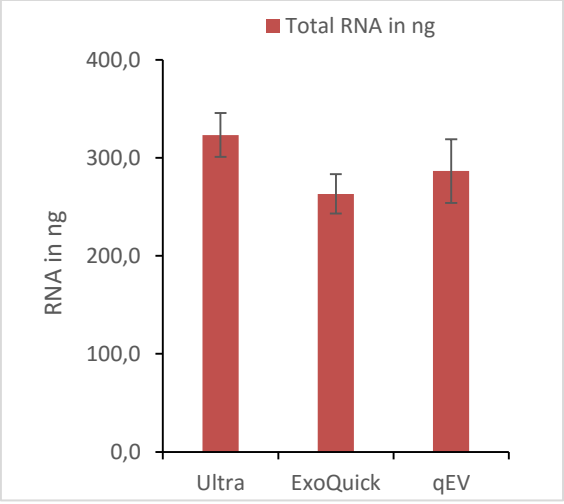

Figure 11 – Total RNA yields obtained from the EVs isolated by ultracentrifugation, ExoQuick kit and qEV SEC columns. RNA extraction was performed using miRCURY kit (Exiqon), and RNA quantification using Nanodrop. Quantity of total RNA is indicated in ng (nanograms). Results are the mean of 6 independent measurements.

In this study, the expression levels of some miRs in EVs isolated by ultracentrifugation, with ExoQuick kit and with the qEV SEC columns were also

compared. In addition, a comparison of these miR levels in EV samples previously treated or not with RNase was also conducted, since it is possible that some miRs can be found outside of the vesicles, as sample contaminants (El-Hefnawy et al., 2004; Arroyo et al., 2011; Turchinovic et al., 2011).

For that, miR-21 (frequently overexpressed in drug resistant cancers) was selected for analysis. In addition, miR-16 was also analysed (as a possible control). However, the analysis of the levels of both miR-21 and miR-16 expressions in the EVs isolated with the different protocols were not analysed in a straightforward way. One of the main problems found was the extremely low amounts of miR-21 and miR-16 detected, in all the EVs isolated from the plasma samples, which meant that their Ct values were outside the standard curve (even with diluted standards). For that reason, the results obtained need to be again repeated, with even more diluted standard curves. Moreover, there is no appropriate internal control miR for exosomes or microvesicles analysis, which would allow the normalization of the results. Several controls have been studied by others, in order to identify an appropriate control for analysis of miRs from plasma EVs. For instance, U6, snoRNA U38B, snoRNA U43, 18S and 5S rRNA have been tested (Hunter et al., 2008; Moldovan et al., 2013), but it was verified that their expressions differ in the plasma EVs from different origins (Hunter et al., 2008), thus none of them has been considered an ideal internal control. In addition, the U6 expression was also shown to be unstable, indicating that the use of U6 may be unsuitable for the normalization of serum EV miR expression (Li et al., 2015). Thus, due to the absence of controls for EVs-miRs normalization, the results of miR-21 and miR-16 expression have been presented using the Ct-values **(Tables 7 and 8)**. Indeed, the fact that all the experiments were performed with equivalent amounts of total RNA (for all the six patients), allowed the analysis of the results using Ct-values in the absence of an internal control (even though this is not ideal).

Thus, even though the results need to be further confirmed with diluted standard curves, the preliminary results obtained indicate that the qEV SEC columns showed the presence of both miR-21 and miR-16 at early Ct values when compared to later Ct values found in the samples obtained from the ultracentrifugation or the ExoQuick kit methods **(Table 7)**. However, levels of miR-21 and miR-16 were also detected in both of the ultracentrifugation and ExoQuick kit isolated EVs **(Table 7)**. Nevertheless, the detection of the mentioned miRs at lower Ct values suggested that higher levels of miRs were isolated by the qEV SEC method. However, to confirm if these miRs were inside the EVs

or from non-vesicular origin, the three methods were compared with prior RNase treatment of samples (in two additional patients, **Table 8**).

With prior RNase treatment, the above mentioned tendency for the presence of higher amounts of mir-21 and mir-16 in the EVs isolated with the qEV SEC columns was not confirmed (Table 8), suggesting that these protocols might isolate non-vesicular or extracellular miRs. This is in agreement with some authors that claim that RNase treatment is essential, to avoid detection of the miRs from non-vesicular origin.

Table 7. miR-21 and miR-16 Ct values in EVs isolated from MM plasma samples (without RNase treatment)

	Samples	***Methods***		
		Ultracentrifugation	***ExoQuick***	***qEV SEC columns***
miR-21 Ct	*EVs Patient 19*	31.3	32.5	26.7
	EVs Patient 20	33.3	32.8	29.9
	EVs Patient 21	33.3	33.5	30.2
	EVs Patient 22	32.5	32.6	29.5
miR-16 Ct	*EVs Patient 19*	32.5	33.1	27.8
	EVs Patient 20	32.8	31.8	29.6
	EVs Patient 21	34.0	33.6	29.7
	EVs Patient 22	34.4	33.3	32.4

Table 8. miR-21 and miR-16 Ct values in EVs isolated from MM plasma samples (with RNase treatment)

	Samples	***Methods***		
		Ultracentrifugation	***ExoQuick***	***qEV SEC columns***
miR-21 Ct	*EVs Patient 18 (RNAse treated)*	35.3	33.1	35.8
	EVs Patient 34 (RNase treated)	34,9	32.9	38.4
miR-16 Ct	*EVs Patient 18 (RNase treated)*	35.3	33.1	34.5
	EVs Patient 34 (RNase treated)	35.3	36.0	36.0

3. Results and Discussion – part II

Selecting bortezomib-resistant MM cell lines

One of the aims of the present study was to select two pairs of bortezomib-resistant cells lines from the sensitive cell lines RPMI-8226 (from peripheral blood) and NCI-H929 (from the bone marrow). With that purpose, the IC_{50} concentrations of bortezomib were initially determined for the RPMI-8226 and NCI-H929 cells. For that, the cell viability was calculated (using the Presto Blue assay) following incubation with different drug concentrations and presented as a percentage of viable cells, compared with untreated controls. Simultaneously, controls treatments were included (wells without cells, containing only medium and the drug were used). As shown in **Figure 12**, the obtained IC_{50} values for bortezomib were approximately 3.17 nM in the RPMI-8226 cell line and 1.48 nM in the NCI-H929 cell line.

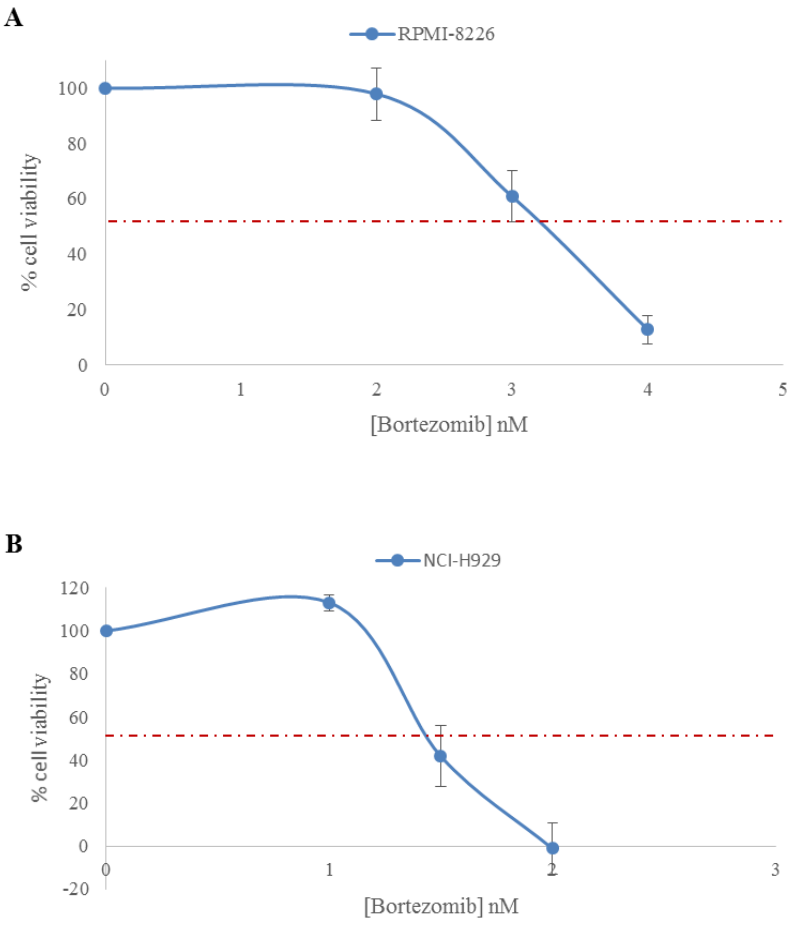

Figure 12 –Dose-response curve of (A) RPMI-8226 cells and (B) NCI-H929 cells to bortezomib. Cells were treated with different bortezomib concentrations and 48h later the cellular viability was assessed using the Presto Blue assay. The half maximal inhibitory concentration (IC50) values were determined: 3.17 nM for the RPMI-8226 cells and 1.48 nM for the NCI-H929 cells. Values are the mean ± S.E. from 3 independent experiences.

Following the determination of the dose-response curves, over a period of six months, stepwise concentrations of bortezomib were added to both cell lines. Cells were initially treated with a low concentration of bortezomib (IC_{25}) which was successively increased until the bortezomib concentration reached approximately twice the IC_{50} concentration. Following that time of drug selection, another dose-response curve was carried out, in order to confirm if the selected cells had become drug-resistant. These dose-response curves were carried out with the resazurin assay. As shown in **Figure 13**, there was only a slight increase in the IC_{50} concentration of bortezomib in both of the selected cells, when compared to the parental cells, suggesting that they only presented a slight increase in drug resistance. One possible explanation for the low increase in drug resistance observed following 6 months of treatment with increasing concentrations of bortezomib may be due to a possible instability of bortezomib. Indeed, it is possible that this drug might have lost its activity during the six month period during which these experiments were carried out.

Therefore, longer periods of drug treatment will be necessary, in order to obtain drug-resistant cells lines. This work will need to be continued in the laboratory.

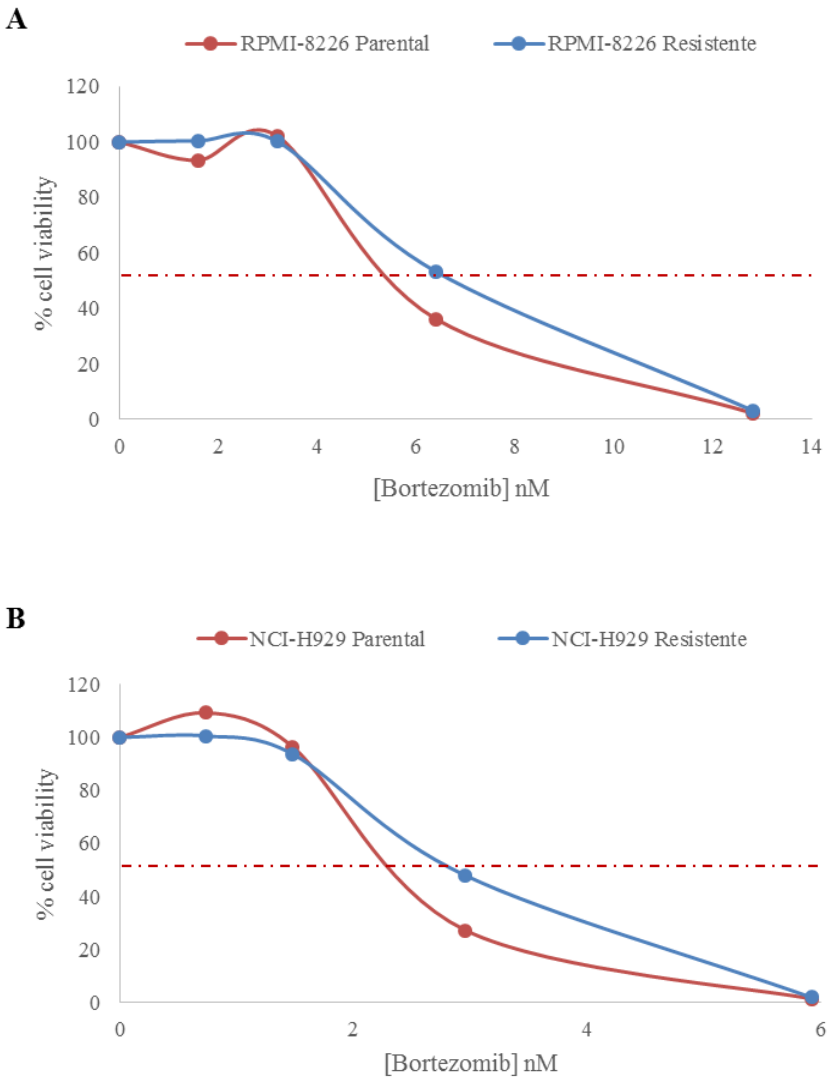

Figure 13 – Dose-response curves to bortezomib of (A) parental and selected for drug resistance RPMI-8226 cells and of (B) parental and selected for drug resistance NCI-H929 cells. Drug response was determined with the Resazurin assay. Drug resistant cells were treated with increasing concentrations of bortezomib during 6 months.

Chapter IV – Conclusion

Conclusion

EVs are potential biomarkers for cancer diagnosis and prognosis, including in MM disease. Despite the major advances in the MM treatment, drug resistance remains a major obstacle to therapeutic success, leading to a high rate of relapse.

In this study, we compared three different methods for isolation of plasma EVs, with the purpose of selecting and optimizing a protocol for a rapid and reproducible isolation of EVs from the plasma of MM patients, which would allow the isolation of EVs from many size ranges (including exosomes and microvesicles). Therefore, it was essential that the selected protocol would provide enough EVs for size characterization, surface markers protein analysis and miRNAs expression studies. The ultracentrifugation, ExoQuick commercial kit and qEV SEC columns were selected, since these methods were based on different principles (centrifugation, precipitation and chromatography).

The ultracentrifugation has been frequently used by other authors as the standard method for EVs isolation. However, it is much more time consuming than the ExoQuick kit or the qEV SEC protocols. Moreover, it allows the extraction of low amounts of protein (possibly due to reduced particle recovery) and requires larger amounts of starting samples (plasma). Finally, it requires the use of expensive equipment. For that reason, it was concluded that it is not a sufficiently fast and efficient protocol for the study of EVs obtained from plasma.

The ExoQuick kit and the qEV SEC columns were found to be quicker and simpler protocols, providing higher amounts of protein (possibly due to more particle recovery) when compared to the ultracentrifugation. However, the size of the EVs isolated with the ExoQuick kit (30 nm to 100 nm) suggests that they were exosomes only; in contrast, the size of the EVs isolated with the qEV SEC protocols (from 100 nm to 1000 nm) suggests that these columns not only isolated exosomes but also microvesicles, as was the initial intention.

All the protocols have provided EVs which presented EV protein markers, without evident co-isolation of cell debris. However, they all isolated albumin (plasma contaminant).

In conclusion, the preferred method was the qEV SEC columns, for providing a quick and efficient protocol for the isolation of EVs with various sizes. However, this

protocol needs further optimization in order to reduce or possibly eliminate the protein contaminants from the plasma.

Finally, preliminary results suggest that the qEV SEC columns allow the detection of higher levels of miR-21 and miR-16, when compared with the other two methods, possibly because this method allows the isolation of different types of EVs. However, these are only preliminary results which need to be confirmed before conclusions can be taken.

References

Abdi, J., Chen, G., and Chang, H. (2013). Drug resistance in multiple myeloma: latest findings and new concepts on molecular mechanisms. Oncotarget *4*, 2186-2207.

Abraham, J., Salama, N.N., and Azab, A.K. (2015). The role of P-glycoprotein in drug resistance in multiple myeloma. Leuk Lymphoma *56*, 26-33.

Agarwal, J.R., and Matsui, W. (2010). Multiple Myeloma: A Paradigm for Translation of the Cancer Stem Cell Hypothesis. Anti-Cancer Agents in Medicinal Chemistry *10*, 116-120.

Albarracin, F., and Fonseca, R. (2011). Plasma cell leukemia. Blood Reviews *25*, 107-112.

Alexander, D.D., Mink, P.J., Adami, H.-O., Cole, P., Mandel, J.S., Oken, M.M., and Trichopoulos, D. (2007). Multiple myeloma: a review of the epidemiologic literature. International journal of cancer Journal international du cancer *120 Suppl 12*, 40-61.

An, G., Xu, Y., Shi, L., Zhong, S., Dend, S., Xie, Z., Sui, W., Zhan, F. and Qiu, L. (2014). Chromosome 1q21 gains confer inferior outcomes in multiple myeloma treated with bortezomib but copy number variation and percentage of plasma cells involved have no additional prognostic value. Haematologica 99(2).

Anderson, K.C. (2005). Lenalidomide and thalidomide: Mechanisms of action - Similarities and differences. Seminars in Hematology *42*, S3-S8.

Arroyo, J.D., Chevillet, J.R., Kroh, E.M., Ruf, I.K., Pritchard, C.C., Gibson, D.F., Mitchell, P.S., Bennett, C.F., Pogosova-Agadjanyan, E.L., Stirewalt, D.L., *et al.* (2011). Argonaute2 complexes carry a population of circulating microRNAs independent of vesicles in human plasma. Proceedings of the National Academy of Sciences of the United States of America *108*, 5003-5008.

Avet-Loiseau, H., Facon, T., Grosbois, B., Magrangeas, F., Rapp, M.J., Harousseau, J.L., Minvielle, S., Bataille, R., and Intergroupe Francophone du, M. (2002). Oncogenesis of multiple myeloma: 14q32 and 13q chromosomal abnormalities are not randomly distributed, but correlate with natural history, immunological features, and clinical presentation. Blood *99*, 2185-2191.

Balsas, P., López-Royuela, N., Galán-Malo, P., Anel., A., Marzo, I., Naval, J. (2009). Cooperation between Apo2L/TRAIL and bortezomib in multiple myeloma apoptosis. Biochemical pharmacology *77*, 804-812.

Baranyai, T., Herczeg, K., Onodi, Z., Voszka, I., Modos, K., Marton, N., Nagy, G., Mager, I., Wood, M.J., El Andaloussi, S., et al. (2015). Isolation of Exosomes from Blood Plasma: Qualitative and Quantitative Comparison of Ultracentrifugation and Size Exclusion Chromatography Methods. PLoS One *10*, e0145686.

Basak, G. W., and Carrier, E. (2010). The Search for Multiple Myeloma Stem Cells: The Long and Winding Road. Biol Blood Marrow Transplant *16*, 587-594.

Bergsagel, P.L., and Kuehl, W.M. (2005). Molecular pathogenesis and a consequent classification of multiple myeloma. Journal of Clinical Oncology *23*, 6333-6338.

Bergsagel, P.L., Mateos, M.V., Gutierrez, N.C., Rajkumar, S.V., and San Miguel, J.F. (2013). Improving overall survival and overcoming adverse prognosis in the treatment of cytogenetically high-risk multiple myeloma. Blood *121*, 884-892.

Bi, C., and Chng, W.J. (2014). MicroRNA: important player in the pathobiology of multiple myeloma. BioMed research international *2014*, 521586-521586.

Bianchi, G. and Munshi, N., (2015). Pathogenesis beyond the cancer clone(s) in multiple myeloma. Blood *125*, 3049-3058.

Boersma-Vreugdenhil, G.R., van Stralen, E., Peeters, T., Michaux, L., Hagemeijer, A., Pearson, P.L., Clevers, H.C., and Bast, B.J.E., (2004) The recurrent t(14;20) in MM results in aberrant expression of MAFB. British Journal of Haematology, 126, 355-363

Boing, A.N., van der Pol, E., Grootemaat, A.E., Coumans, F.A., Sturk, A., and Nieuwland, R. (2014). Single-step isolation of extracellular vesicles by size-exclusion chromatography. J Extracell Vesicles *3*.

Boyd, K.D., Ross, F.M., Tapper, W.J., Chiecchio, L., Dagrada, G., Konn, Z. J. et al (2011) The clinical impact and molecular biology of del(17p) in Multiple Myeloma treated with conventional Thalidomide-based therapy. Gene, Chromosomes & Cancer 50:765-774.

Brito, J.L., Walker, B., Jenner, M., Dickens, N.J., Brown, N.J., Ross, F.M., Avramidou, A., Irving, J.A., Gonzalez, D., Davies, F.E., et al. (2009). MMSET deregulation affects cell cycle progression and adhesion regulons in t(4;14) myeloma plasma cells. Haematologica *94*, 78-86.

Burger, R., Le Gouill, S., Tai, Y., Shringarpure, R., Tassone, P., Neri, P., Podar, K., Catley, L., Hideshima, T., Chauhan, et al. (2009). Janus kinase inhibitor INCB20 has antiproliferative and apoptotic effects on human myeloma cells in vitro and in vivo. Molecular Cancer Therapeutics *8(1)*, 26-35.

Caby, M.P., Lankar, D., Vincendeau-Scherrer, C., Raposo, G., and Bonnerot, C. (2005). Exosomal-like vesicles are present in human blood plasma. International immunology *17*, 879-887.

Catlett-Falcone, R., Landowski, T.H., Oshiro, M.M., Turkson, J., Levitzki, A., Savino, R., Ciliberto, G., Mosciniski, L., et al. (1999). Constitutive activation of Stat3 signaling confers resistance to apoptosis in human U266 myeloma cells. Immunity *10*, 105-115.

Chatterjee, M., Jain, S., Stuhmer, T., Andrulis, M., Ungethum, U., Kuban, R., Lorentz, H., Bommert, K., et al. (2007).STAT3 and MAPK signaling maintain overexpression of heat shock proteins 90 and in multiple myeloma cells, which critically contribute to tumor-cell survival. Blood *109*, 720-728.

Chatterjee, M., Andrulis, M., Stuhmer, T., Muller, E., Hofmann, C., Steinbrunn, T., Heimberger, T., Schraud, H., Kressmann, S., Einsele, H., et al. (2013). The PI3K/Akt signaling pathway regulates the expression of Hsp70, which critically contributes to Hsp90-chaperone function and tumor cell survival in multiple myeloma. Haematologica *98*, 1132-1141.

Chauhan, D., Uchiyama, H., Akbarali, Y., Urashima, M., Yamamoto, K., Libermann, T.A., and Anderson, K.C. (1996). Multiple Myeloma cell adhesion-induced interleukin-6 expression in bone marrow stromal cells involves cctivation of NF-KB. Blood *87*, 1104-1112.

Chen, D., Frezza, M., Schmitt, S., Kanwar, J., and Dou, Q.P. (2011). Bortezomib as the First Proteasome Inhibitor Anticancer Drug: Current Status and Future Perspectives. Current Cancer Drug Targets *11*, 239-253.

Chen, X., Liang, H., Zhang, J., Zen, K., and Zhang, C.-Y. (2012). Horizontal transfer of microRNAs: molecular mechanisms and clinical applications. Protein & Cell *3*, 28-37.

Chen, W.-x., Liu, X.-m., Lv, M.-m., Chen, L., Zhao, J.-h., Zhong, S.-l., Ji, M.-h., Hu, Q., Luo, Z., Wu, J.Z., et al. (2014). Exosomes from Drug-Resistant Breast Cancer Cells Transmit Chemoresistance by a Horizontal Transfer of MicroRNAs. Plos One *9*.

Cheng, L., Sharples, R.A., Scicluna, B.J., and Hill, A.F. (2014). Exosomes provide a protective and enriched source of miRNA for biomarker profiling compared to intracellular and cell-free blood. J Extracell Vesicles *3*.

Chesi, M., Bergsagel, P.L., Shonukan, O.O., Martelli, M.L., Brents, L.A., Chen, T., Schrock, E., Ried, T., and Kuehl, V.M. (1998). Frequent dysregulation of the c-maf proto-oncogene at 16q23 by translocation to an Ig locus in multiple myeloma. Blood *91*, 4457-4463.

Chesi, M., Brents, L., A., Ely, S. A., Bais, C., Robbiani, D.F., Mesri, E.A., Kuehl, W.L and Bergsagel, P.L. (2001). Activated fibroblast growth factor receptor 3 is an oncogene that contributes to tumor progression in multiple myeloma. Blood *97*, 729-736.

Dalton, W.S. (1997). Detection of multidrug resistance gene expression in multiple myeloma. Leukemia *11*, 1166-1169.

Damiano, J.S., Cress, A.E., Hazlehurst, L.A., Shtil, A.A and Dalton, W.S. (1999). Cell adhesion mediated drug resistance (CAM-DR): Role of integrins and resistance to apoptosis in human myeloma cell lines. Blood 93, 1658-1667.

Derksen, P.W., Tjin, e., Meijer, H.P. et al (2004) Illegitimate WNT signaling promotes proliferation of multiple myeloma cells. Proc Natl Acad Sci USA 101:6122-6127.

Dimopoulos, M.A., Kastritis, E., Christoulas, D., Migkou, M., Gavriatopoulou, M., Gkotzamanidou, M., Iakovaki, M., Matsouka, C., Mparmparoussi, D., Roussou, M., et al. (2010). Treatment of patients with relapsed/refractory multiple myeloma with lenalidomide and dexamethasone with or without bortezomib: prospective evaluation of the impact of cytogenetic abnormalities and of previous therapies. Leukemia *24*, 1769-1778.

Dimopoulos, K., Gimsing, P., and Gronbaek, K. (2013). Aberrant microRNA expression in multiple myeloma. European Journal of Haematology *91*, 95-105.

El-Hefnawy, T., Raja, S., Kelly, L., Bigbee, W.L., Kirkwood, J.M., Luketich, J.D., and Godfrey, T.E. (2004). Characterization of amplifiable, circulating RNA in plasma and its potential as a tool for cancer diagnostics. Clinical chemistry *50*, 564-573.

Elnenaei, M.O., Grusszka-Westwood, A.M., A'Hern, R., Matutes, E., Sirohi, B., Powles, R., Catovski., D. (2003). Gene abnormalities in multiple myeloma; the relevance of TP53, MDM2, and CDKN2A (2003). Haematologica 2003; 88:539-537.

Falcone, G., Felsani, A., and D'Agnano, I. (2015). Signaling by exosomal microRNAs in cancer. Journal of Experimental & Clinical Cancer Research 34.

Fonseca, R., Barlogie, B., Bataille, R., Bastard, C., Bergsagel, P.L., Chesi, M., Davies, F.E., Drach, J., Greipp, P.R., Kirsch, I.R., et al. (2004). Genetics and cytogenetics of multiple myeloma: a workshop report. Cancer Res *64*, 1546-1558.

Franqui-Machin, R., Wendlandt, E.B., Janz, S., Zhan, F., and Tricot, G. (2015). Cancer stem cells are the cause of drug resistance in multiple myeloma: fact or fiction? Oncotarget *6*, 40496-40506.

Gabrea, A., Berysagel, P.L., and Kuehl, W.M. (2006). Distinguishing primary and secondary translocations in multiple myeloma. DNA Repair *5*, 1225-1233.

Ge, N. and Rudikoff, S. (2000). Insulin-like growth factor I is a dual effector of multiple myeloma cell growth. Blood *96*, 2856-2861.

Gertz, M.A., Lacy, M.q., Dispenzieri, A., Greipp, p.r., Litzow, M.R., et al. (2005). Clinical implication of t(11;14)(q13;q32), t(4;14)(p16.3;q32), and-17p13 in myeloma patients with high-doe therapy. Blood 106:2837-2840

Ghobrial, I.M., Witzig, T.E., and Adjei, A.A. (2005). Targeting apoptosis pathways in cancer therapy. Ca-a Cancer Journal for Clinicians *55*, 178-194.

Ghosh, N., and Matsui, W. (2009). Cancer stem cells in multiple myeloma. Cancer Letters *277*, 1-7.

Gottesman, M.M. (2002). Mechanisms of cancer drug resistance. Annual Review of Medicine *53*, 615-627.

Grogan, T.M., Spier, C.M., Salmon, S.E., Matzner, M., Rybski, J., Weinstein, R.S., Scheper, R.J., and Dalton, W.S. (1993). P-glycoprotein expression in human plasma cell myeloma: correlation with prior chemotherapy. Blood *81*, 490-495.

Guo, Y., Xu, F., Lu, T.J., Duan, Z. and Zhang, Z. (2012). Interleukin-6 signaling pathway in targeted therapy for cancer. Cancer Treatment Reviews *38*, 904–910.

Hamburger, A.W., and Salmon, S.E. (1977). Primary bioassay of human tumor stem cells. Science *197*, 461-463.

Hanamura, I., Iida, S., Akano, Y., Hayami, Y., Kato, M., Miura, K., Harada, S., Banno, S., et al., (2001) Ectopic expression of MAFB gene in human myeloma cells carrying (14;20)(q32;q11) chromosomal translocations. JOURNAL OF Cancer Research 9992,,, 638-644.

Harousseau, J.L., Dreyling, M., and Grp, E.G.W. (2010). Multiple myeloma: ESMO Clinical Practice Guidelines for diagnosis, treatment and follow-up. Annals of Oncology *21*, v155-v157.

Harousseau, J.L. (2012). How to select among available options for the treatment of multiple myeloma. Annals of Oncology *23*, 334-338.

Harshman, S.W., Canella, A., Ciarlariello, P.D., Agarwal, K., Branson, O.E., Rocci, A., Cordero, H., Phelps, M.A., Hade, E.M., Dubovsky, J.A., et al. (2016). Proteomic characterization of circulating extracellular vesicles identifies novel serum myeloma associated markers. Journal of proteomics *136*, 89-98.

Hideshima, T., Chauhan, D., Shima, Y., Raje, N., Davies, F.E., Tai, Y.T., Treon, S.P., Lin, B., Schlossman, R.L., Richardson, P., et al. (2000). Thalidomide and its analogs overcome drug resistance of human multiple myeloma cells to conventional therapy. Blood *96*, 2943-2950.

Hideshima, T., Richardson, P., Chauhan, D., Palombella, V.J., Elliott, P.J., Adams, J. and Anderson, K.C. (2001). The proteasome inhibitor PS-341 inhibits growth, induces apoptosis, and overcomes drug resistance in human multiple myeloma cells. Cancer Research *61*, 3071–3076.

Hideshima, T., Chauhan, D., Richardson, P., Mitsiades, C., Mitsiades, N., Hayashi, T., Munshi, N., Dang, L., Castro, A. et al. (2002). NF-kB as a therapeutic target in multiple myeloma. The Journal of Biochemical Chemistry *277*, 16639–16647.

Hideshima, T., Mitsiades, C., Tonon, G., Richardson, P.G., and Anderson, K.C. (2007). Understanding multiple myeloma pathogenesis in the bone marrow to identify new therapeutic targets. Nature Reviews Cancer *7*, 585-598.

Hong, C.S., Funk, S., Muller, L., Boyiadzis, M., and Whiteside, T.L. (2016). Isolation of biologically active and morphologically intact exosomes from plasma of patients with cancer. J Extracell Vesicles *5*, 29289.

Huff, C.A. and Matsui, W. (2008).Multiple myeloma cancer stem cells. J Clin Oncol. *26(17)*, 2895–2900.

Hurt, E.M., Wiestner, A, Rosenwald, A., Shaffer, A.L., Campo, E., Grogan, T., Bergsagel, P.L., Kuehl, W.M., Staudt, L.M. (2004). Overexpression of c-maf is a frequent oncogenic event in multiple myeloma
that promotes proliferation and pathological interactions with bone marrow stroma. Cancer Cell 2004; 5:191-9

Hunter, M.P., Ismail, N., Zhang, X., Aguda, B.D., Lee, E.J., Yu, L., Xiao, T., Schafer, J., Lee, M.-L.T., Schmittgen, T.D., et al. (2008). Detection of microRNA Expression in Human Peripheral Blood Microvesicles. Plos One *3*.

Huston, A., Leleu, X., Jia, X., Moreau, A.S., Ngo, H.T., Runnels, J., Anderson, J., Alsayed, Y., Roccaro, A., Vallet, S., et al. (2008). Targeting Akt and heat shock protein 90 produces synergistic multiple myeloma cell cytotoxicity in the bone marrow microenvironment. Clinical cancer research : an official journal of the American Association for Cancer Research *14*, 865-874.

Ishii, T., Seike, T., Nakashima, T., Juliger, S., Maharaj, L., Soga, S., Akinaga, S., Cavenagh, J., Joel, S., and Shiotsu, Y. (2012). Anti-tumor activity against multiple myeloma by combination of KW-2478, an Hsp90 inhibitor, with bortezomib. Blood cancer journal *2*, e68.

Ito, T., Ando, H., Suzuki, T., Ogura, T., Hotta, K., Imamura, Y., Yamaguchi, Y., and Handa, H. (2010). Identification of a primary target of thalidomide teratogenicity. Science *327*, 1345-1350.

Jourdan, M., Veyrune, J., De Vos, J., Redal, N., Couderc, G. and Klein, B (2003). A major role for Mcl-1 antiapoptotic protein in the IL-6-induced survival of human myeloma cells. Oncogene *22*, 2950–2959.

Juliano, R.L., and Ling, V. (1976). Surface glycoprotein modulating drug permeability in chinese-hamster ovary cell mutants. Biochimica Et Biophysica Acta *455*, 152-162.

Jundt, F., Probsting, K.S., Anagnostopoulos, I., Muehlinghaus, G., Chatterjee, M., Mathas, S., Bargou, R.C., Manz, R., Stein, H., and Dorken, B. (2004). Jagged1-induced Notch signaling drives proliferation of multiple myeloma cells. Blood *103*, 3511-3515.

Kalff, A. and Spencer, A. (2012).The t(4;14) translocation and FGFR3 overexpression in multiple myeloma: prognostic implications and current clinical strategies. Blood Cancer Journal *2*, e89.

Keats, J.J., Chesi, M., Egan, J.B., Garbitt, V.M., Palmer, S.E., Braggio, E., Van Wier, S., Blackburn, P.R., Baker, A.S. et al. (2012). Clonal competition with alternating dominance in multiple myeloma. Blood *120*, 1067-1076.

Kellner, J., Liu, B. and Li, Z., (2013) Fact or fiction - identifying the elusive multiple myeloma stem cell. Journal of Hematology & Oncology 6:91.

Keifer, J.A., Guttridge, D.C., Ashburner, B.P. and Baldwin, A.S., (2001). Inhibition of NF-kB activity by thalidomide through suppression of IkB kinase activity. The Journal of Biochemical Chemistry *276*, 22382–22387.

Khan, S., Jutzy, J.M., Valenzuela, M.M., Turay, D., Aspe, J.R., Ashok, A., Mirshahidi, S., Mercola, D., Lilly, M.B., and Wall, N.R. (2012). Plasma-derived exosomal survivin, a plausible biomarker for early detection of prostate cancer. PLoS One *7*, e46737.

Khong, T., and Spencer, A. (2011). Targeting HSP 90 induces apoptosis and inhibits critical survival and proliferation pathways in multiple myeloma. Molecular cancer therapeutics *10*, 1909-1917.

Kotla, V., Goel, S., Nischal, S., Heuck, C., Vivek, K., Das, B., and Verma, A. (2009). Mechanism of action of lenalidomide in hematological malignancies. Journal of Hematology & Oncology *2*, 10.

Kowal, J., Arras, G., Colombo, M., Jouve, M., Morath, J.P., Primdal-Bengtson, B., Dingli, F., Loew, D., Tkach, M., and Thery, C. (2016). Proteomic comparison defines novel markers to characterize heterogeneous populations of extracellular vesicle subtypes. Proc Natl Acad Sci U S A *113*, E968-977.

Kronke, J., Udeshi, N.D., Narla, A., Grauman, P., Hurst, S.N., McConkey, M., Svinkina, T., Heckl, D., Comer, E., Li, X., et al. (2014). Lenalidomide causes selective degradation of IKZF1 and IKZF3 in multiple myeloma cells. Science *343*, 301-305.

Kuehl, W.M., and Bergsagel, P.L. (2002). Multiple myeloma: Evolving genetic events and host interactions. Nature Reviews Cancer *2*, 175-187.

Kumar, S.K., Dispenzieri, A., Lacy, M.Q., Gertz, M.A., Buadi, F.K., Pandey, S., Kapoor, P., Dingli, D., Hayman, S.R., Leung, N., et al. (2014). Continued improvement in survival in multiple myeloma: changes in early mortality and outcomes in older patients. Leukemia *28*, 1122-1128.

Kumar, S.K., Rajkumar, S.V., Dispenzieri, A., Lacy, M.Q., Hayman, S.R., Buadi, F.K., Zeldenrust, S.R., Dingli, D., Russell, S.J., Lust, J.A., et al. (2008). Improved survival in multiple myeloma and the impact of novel therapies. Blood *111*, 2516-2520.

Kyle, R.A., and Rajkumar, S.V. (2008). Multiple myeloma. Blood *111*, 2962-2972.

Kyle, R.A., and Rajkurnar, S.V. (2009). Treatment of Multiple Myeloma: A Comprehensive Review. Clinical Lymphoma & Myeloma *9*, 278-288.

Lagrue, K., Carisey, A., Morgan, D.J., Chopra, R., and Davis, D.M. (2015). Lenalidomide augments actin remodeling and lowers NK-cell activation thresholds. Blood *126*, 50-60.

Le Gouill, S., Podar, K., Harousseau, J.L., Anderson, K.C. (2004) a. Mcl-1 regulation and its role in multiple myeloma. Cell Cycle *3(10),*1259-62

Le Gouill, S., Podar, K, Amiot, M., Hideshima, T., Chauhan, D. et al. (2004) b. VEGF induces Mcl-1 up-regulation and protects multiple myeloma cells against apoptosis. Blood *104(9)*, 2886-2892.

Lee, Y., El Andaloussi, S., and Wood, M.J.A. (2012). Exosomes and microvesicles: extracellular vesicles for genetic information transfer and gene therapy. Human Molecular Genetics 21, R125-R134.

Lentzsch, S., Chatterjee, M., Gries, M., Bommert, K., Gollasch, H., Dorken, B. and Bargou, R.C. (2004). PI3-K/AKT/FKHR and MAPK signaling cascades are redundantly stimulated by a variety of cytokines and contribute independently to proliferation and survival of multiple myeloma cells. Leukemia *18*, 1883–1890.

Leone, E., Morelli, E., Di Martino, M.T., Amodio, N., Foresta, U., Gullà, A. et al., (2013). Targeting miR-21 inhibits in vitro and in vivo multiple myeloma cell growth. Clin Cancer Res *19(8)*, 2096–2106.

Li, J., Favata, M., Kelley, J.A., Caulder, E., Thomas, B., Wen, X., Sparks, R.B., Arvanitis, A., Rogers, J.D. et al. (2010). INCB16562, a JAK1/2 selective inhibitor, is efficacious against multiple myeloma cells and reverses the protective effects of cytokine and stromal cell support. Neoplasia *12*, 28-38

Li, Y., Zhang, L., Liu, F., Xiang, G., Jiang, D., and Pu, X. (2015). Identification of endogenous controls for analyzing serum exosomal miRNA in patients with hepatitis B or hepatocellular carcinoma. Disease markers *2015*, 893594.

Lin, B., Podar, K., Gupta, D., Tai, Y., Li, S., Weller, E., Hideshima, T., Lentzsch, S., et al. (2002). The vascular endothelial growth factor receptor tyrosine kinase inhibitor PTK787/ZK222584 inhibits growth and migration of multiple myeloma cells in the bone marrow microenvironment. Cancer Research *62*, 5019–5026.

Lobb, R.J., Becker, M., Wen, S.W., Wong, C.S., Wiegmans, A.P., Leimgruber, A., and Moller, A. (2015). Optimized exosome isolation protocol for cell culture supernatant and human plasma. J Extracell Vesicles *4*, 27031.

Lodé, L., Eveillard,. M., Trichet, V., Soussi, T., Wuillème, S., Richebourg, S., Magrangeas, F., et al (2010). Mutations in TP53 are exclusively associated with del(17p) in multiple myeloma. Haematologica 95(11).

Loffler, D., Brocke-Heidrich, K., Pfeifer, G., Stocsits, C., Hackermuller, J., Kretzschmar,A.K., Burger, R., Gramatzki, M., et al. (2007). Interleukin-6–dependent survival of multiple myeloma cells involves the Stat3-mediated induction of microRNA-21 through a highly conserved enhancer. Blood *110*, 1330-1333.

Lopes-Rodrigues, V., Di Luca, A., Sousa, D., Seca, H., Meleady, P., Henry, M., Lima, R.T., O'Connor, R., and Vasconcelos, M.H. (2016). Multidrug resistant tumour cells shed more microvesicle-like EVs and less exosomes than their drug-sensitive counterpart cells. Biochim Biophys Acta *1860*, 618-627.

Lu, G., Middleton, R.E., Sun, H., Naniong, M., Ott, C.J., Mitsiades, C.S., Wong, K.K., Bradner, J.E., and Kaelin, W.G., Jr. (2014). The myeloma drug lenalidomide promotes the cereblon-dependent destruction of Ikaros proteins. Science *343*, 305-309.

Matsui, W., Huff, C.A., Wang, Q.J., Malehorn, M.T., Barber, J., Tanhehco, Y., Smith, B.D., Civin, C.I., and Jones, R.J. (2004). Characterization of clonogenic multiple myeloma cells. Blood *103*, 2332-2336.

Matsui, W., Wang, Q., Barber, J.P., Brennan, S., Smith, B.D., Borrello, I., McNiece, I., Lin, L., Ambinder, R.F., Peacock, C., et al. (2008). Clonogenic multiple myeloma progenitors, stem cell properties, and drug resistance. Cancer Research *68*, 190-197.

Meads, M.B., Gatenby, R.A. and Dalton, W.S. (2009). Environment-mediated drug resistance: a major contributor to minimal residual disease. Nature Reviews *9*, 665-674.

Minciacchi, V.R., Freeman, M.R., and Di Vizio, D. (2015). Extracellular Vesicles in Cancer: Exosomes, Microvesicles and the Emerging Role of Large Oncosomes. Seminars in Cell & Developmental Biology 40, 41-51.

Mitsiades, C.S., Treon, S.P., Mitsiades, N., Shima, Y., Richardson, P., Schlossman, R., Hideshima, T. and Anderson, K.C. (2001). TRAIL/Apo2L ligand selectively induces apoptosis and overcomes drug resistance in multiple myeloma: therapeutic applications. Blood *98*,795-804.

Mitsiades, C.S., Mitsiades, N., Munshi, N.C., and Anderson, K.C. (2004). Focus on multiple myeloma. Cancer Cell *6*, 439-444.

Mitsiades, C.S., Mitsiades, N.S., McMullan, C.J., Poulaki, V., Kung, A.L., Davies, F.E., Morgan, G., Akiyama, M., Shringarpure, R., Munshi, N.C., et al. (2006). Antimyeloma activity of heat shock protein-90 inhibition. Blood *107*, 1092-1100.

Mohty, M., Malard, F., Mohty, B., Savani, B., Moreau, P., and Terpos, E. (2014). The effects of bortezomib on bone disease in patients with multiple myeloma. Cancer *120*, 618-623.

Moldovan, L., Batte, K., Wang, Y., Wisler, J., and Piper, M. (2013). Analyzing the circulating microRNAs in exosomes/extracellular vesicles from serum or plasma by qRT-PCR. Methods in molecular biology *1024*, 129-145.

Momen-Heravi, F., Balaj, L., Alian, S., Tigges, J., Toxavidis, V., Ericsson, M., Distel, R.J., Ivanov, A.R., Skog, J., and Kuo, W.P. (2012). Alternative methods for characterization of extracellular vesicles. Frontiers in physiology *3*, 354.

Monaghan. K. A., Khong, T., Burns, C.J., and Spencer, A. (2011). The novel JAK inhibitor CYT387 suppresses multiple signalling pathways, prevents proliferation and induces apoptosis in phenotypically diverse myeloma cells. Leukemia *25*, 1891–1899.

Moreau, P., Attal, M., and Facon, T. (2015). Frontline therapy of multiple myeloma. Blood *125*, 3076-3084.

Morgan, G.J., Walker, B.A., and Davies, F.E. (2012). The genetic architecture of multiple myeloma. Nature Reviews Cancer *12*, 335-348.

Muller, L., Hong, C.-S., Stolz, D.B., Watkins, S.C., and Whiteside, T.L. (2014). Isolation of biologically-active exosomes from human plasma. Journal of Immunological Methods *411*, 55-65.

Nemec, P., Zemanova, Z., Greslikova, H., et al. (2010). Gain of 1q21 is an unfavorable genetic prognostic factor for multiple myeloma patients treated with high-dose chemotherapy. Biol Blood Marrow Transplant. 16(4):548–554.

Ngo, B.T., Felthaus, j., Hein, M., Follo, M., Wider, D., Ihorst, G., Engelhardt, M., and Wasch, R. (2010). Monitoring bortezomib therapy in multiple myeloma: screening of cyclin D1, D2, and D3 via reliable real-time polymerase chain reaction and association with clinico-pathological features and outcome. Leukemia & Lymphoma 51(9): 1632-1642

Ni, H., Ergin, M., Huang, Q. Qin, J., Amin, H.M., Martinez, R.L., Saeed, S. et al. (2001). Analysis of expression of nuclear factor kB (NF-kB) in multiple myeloma: downregulation of NF-kB induces apoptosis. British Journal of Haematology *115*, 279-286

Nishida-Aoki, N., and Ochiya, T. (2015). Interactions between cancer cells and normal cells via miRNAs in extracellular vesicles. Cellular and Molecular Life Sciences 72, 1849-1861.

Nooter, K., and Sonneveld, P. (1994). Clinical relevance of P-glycoprotein expression in haematological malignancies. Leukemia research *18*, 233-243.

Nooter, K., and Stoter, G. (1996). Molecular mechanisms of multidrug resistance in cancer chemotherapy. Pathology Research and Practice *192*, 768-780.

O'Connor, R., Ooi, M.G., Meiller, J., Jakubikova, J., Klippel, S., Delmore, J., Richardson, P., Anderson, K., Clynes, M., Mitsiades, C.S., et al. (2013). The interaction of bortezomib with multidrug transporters: implications for therapeutic applications in advanced multiple myeloma and other neoplasias. Cancer Chemotherapy and Pharmacology *71*, 1357-1368.

Palumbo, A., and Anderson, K. (2011). MEDICAL PROGRESS Multiple Myeloma. New England Journal of Medicine *364*, 1046-1060.

Palumbo, A., Bringhen, S., Ludwig, H., Dimopoulos, M.A., Blade, J., Mateos, M.V., Rosinol, L., Boccadoro, M., Cavo, M., Lokhorst, H., et al. (2011). Personalized therapy in multiple myeloma according to patient age and vulnerability: a report of the European Myeloma Network (EMN). Blood *118*, 4519-4529.

Pandey MK, A.S., Zangari M, Talamo G. (2015). Drug Resistance in Multiple Myeloma: How to Cross the Border. Annals of Hematology & Oncology *2*, 1025.

Park, C.H., Bergsagel, D.E., and McCulloch, E.A. (1971). Mouse myeloma tumor stem cells: a primary cell culture assay. J Natl Cancer Inst *46*, 411-422.

Peacock, C.D, Wang, Q., Gesell, G.S., Corcoran-Schwartz, I.M., Jones, E., Kim, J., et al. (2007). Hedgehog signaling maintains a tumor stem cell compartment in multiple myeloma. PNAS *104*, 4048–4053.

Pichiorri, F., De Luca, L., and Aqeilan, R.I. (2011). MicroRNAs: New Players in Multiple Myeloma. Frontiers in genetics *2*, 22-22.

Podar, K.., Tai, Y., Davies, F.E., Lentzsch, S., Sattler, M., Hideshima, T., Lin, B.K. et al. (2001). Vascular endothelial growth factor triggers signaling cascades mediating multiple myeloma cell growth and migration. Blood *98*,428-435.

Podar, K., Tonon, G., Sattler, M., Tai, Y., LeGouill, S., Yasui, H., Ishitsuka, K. et al. (2006). The small-molecule VEGF receptor inhibitor pazopanib (GW786034B) targets both tumor and endothelial cells in multiple myeloma. PNAS *103*, 19478–19483.

Qazilbash, M.H., Saliba, R.M., Ahmed, B., Parikk, G., Mendoza, U.P., et al., (2007). Deletion of the short arm of chromosome I (del1p) is a strong predictor of poor outcome in myeloma patients undergoing an autotransplant. Biology of blood and marrow transplantation 13:1066-1072.

Raab, M.S., Podar, K., Breitkreutz, I., Richardson, P.G., and Anderson, K.C. (2009). Multiple myeloma. Lancet *374*, 324-339.

Rajan, A.M., and Rajkumar, S.V. (2015). Interpretation of cytogenetic results in multiple myeloma for clinical practice. Blood cancer journal *5*, e365.

Rajkumar, S.V. (2009). Multiple Myeloma. Current Problems in Cancer *33*, 7-64.

Rajkumar, S.V. (2011). Treatment of multiple myeloma. Nature Reviews Clinical Oncology *8*, 479-491.

Rajkumar, S.V. (2012). Multiple myeloma: 2012 update on diagnosis, risk-stratification, and management. American Journal of Hematology *87*, 79-88.

Rajkumar, S.V., Dimopoulos, M.A., Palumbo, A., Blade, J., Merlini, G., Mateos, M.V., Kumar, S., Hillengass, J., Kastritis, E., Richardson, P., et al. (2014). International Myeloma Working Group updated criteria for the diagnosis of multiple myeloma. Lancet Oncology *15*, E538-E548.

Raposo, G., and Stoorvogel, W. (2013). Extracellular vesicles: Exosomes, microvesicles, and friends. Journal of Cell Biology 200, 373-383.

Reece, D., Song, K.W., Fu, T., Roland, B., Chang, h., Horsman, D.E., Mansoor, A., Chen, C., et al., (2009) Influence of cytogenetics in patients with relapsed or refractory multiple myeloma treated with lenalidomide plus dexamethasone: adverse effect of deletion 17p13. Blood 114:522-525.

Richardson, P., Jagannath, S., Hussein, M., Berenson, J., Singhal, S., Irwin, D., Williams, S.F., Bensinger, W., Badros, A.Z., Vescio, R., et al. (2009). Safety and efficacy of single-agent lenalidomide in patients with relapsed and refractory multiple myeloma. Blood *114*, 772-778.

Richardson, P.G., Barlogie, B., Berenson, J., Singhal, S., Jagannath, S., Irwin, D., Rajkumar, S.V., Srkalovic, G., Alsina, M., Alexanian, R., et al. (2003). A phase 2 study of bortezomib in relapsed, refractory myeloma. New England Journal of Medicine *348*, 2609-2617.

Roccaro, A.M., Hideshima, T., Raje, N., Kumar, S., Ishitsuka, K., Yasui, H., Shiraishi, N., Ribatti, D., Nico, B., Vacca, A., et al. (2013). Bortezomib mediates antiangiogenesis in multiple myeloma via direct and indirect effects on endothelial cells. Cancer Research *66*, 184-191.

Rocci, A., Hofmeister, C.C., and Pichiorri, F. (2014). The potential of miRNAs as biomarkers for multiple myeloma. Expert Review of Molecular Diagnostics *14*, 947-959.

Ross, F.M., Chiecchio, L., Dagrada, G., Protheroe, R.K., Stockley, D.M., Harrison, C.J., Cross, N.C., Szubert, A.J., Drayson, M.T., Morgan, G.J., et al. (2010). The t(14;20) is a poor prognostic factor in myeloma but is associated with long-term stable disease in monoclonal gammopathies of undetermined significance. Haematologica *95*, 1221-1225.

Sagaster, V., Ludwig, H., Kaufmann, H., Odelga, V., Zojer, N., Ackermann, J., Kuenburg, E., Wieser, R., Zielinski, C., and Drach, J. (2007). Bortezomib in relapsed multiple myeloma: response rates and duration of response are independent of a chromosome 13q-deletion. Leukemia *21*, 164-168.

Saltarella, I., Lamanuzzi, A., Reale, A., Vacca, A. and Ria, R. (2015). Identify multiple myeloma stem cells: Utopia? World J Stem Cells *7*, 84-95.

San Miguel, J.F., Schlag, R., Khuageva, N.K., Dimopoulos, M.A., Shpilberg, O., Kropff, M., Spicka, I., Petrucci, M.T., Palumbo, A., Samoilova, O.S., et al. (2008). Bortezomib plus melphalan and prednisone for initial treatment of multiple myeloma. New England Journal of Medicine *359*, 906-917.

Seidl, S., Kaufmann, H., and Drach, J. (2003). New insights into the pathophysiology of multiple myeloma. Lancet Oncology *4*, 557-564.

Sekiguchi, N., Outsubo, K, Wagatsuma, M., Midorikawa, K., Nagata, A., Noto, S., Yamada, K., Takezako. and N. (2014). The impact of c-Myc gene-related aberrations in newly diagnosed myeloma with bortezomib/dexamethasone therapy. Int J Hematol 99:288-295.

Shaughnessy Jr, J., Gabre, A., Qi, Y., Brents, L., Zhan, F., Tian, E., Sawyer, J., Barlogie, B., Bergsagel, P.L., and Kuehl, M., () Cyclin D3 at 6p21 is dysregulated by recurrent chromosomal translocations to immunoglobulin loci in multiple myeloma. Blood 98:217-223.

Sewify, E.M., Afifi, O.A., Mosad, E., Zaki, A.H., and El Gammal, S.A. (2014). Cyclin D1 amplification in multiple myeloma is associated with multidrug resistance expression. Clinical lymphoma, myeloma & leukemia *14*, 215-222.

Sirohi, B., and Powles, R. (2004). Multiple myeloma. Lancet *363*, 875-887.

Smadja, N.V., Bastard, C., Brigaudeau, C., Leroux, D., Fruchart, C., and Grp Francais Cytogenetique, H. (2001). Hypodiploidy is a major prognostic factor in multiple myeloma. Blood *98*, 2229-2238.

Sodar, B.W., Kittel, A., Paloczi, K., Vukman, K.V., Osteikoetxea, X., Szabo-Taylor, K., Nemeth, A., Sperlagh, B., Baranyai, T., Giricz, Z., et al. (2016). Low-density lipoprotein mimics blood plasma-derived exosomes and microvesicles during isolation and detection. Scientific reports *6*, 24316.

Szatanek, R., Baran, J., Siedlar, M., and Baj-Krzyworzeka, M. (2015). Isolation of extracellular vesicles: Determining the correct approach (Review). International journal of molecular medicine *36*, 11-17.

Talley, P.J., Chantry, A.D., and Buckle, C.H. (2015). Genetics in myeloma: genetic technologies and their application to screening approaches in myeloma. British Medical Bulletin *113*, 15-30.

Tamaki, A., Ierano, C., Szakacs, G., Robey, R.W., and Bates, S.E. (2011). The controversial role of ABC transporters in clinical oncology. In Essays in Biochemistry: Abc Transporters, F.J. Sharom, ed. (London: Portland Press Ltd), pp. 209-232.

Thery, C., Amigorena, S., Raposo, G., and Clayton, A. (2006). Isolation and characterization of exosomes from cell culture supernatants and biological fluids. Current protocols in cell biology / editorial board, Juan S Bonifacino [et al] *Chapter 3*, Unit 3 22.

Thomas, H., and Coley, H.M. (2003). Overcoming multidrug resistance in cancer: an update on the clinical strategy of inhibiting p-glycoprotein. Cancer control : journal of the Moffitt Cancer Center *10*, 159-165.

Tsuruo, T., Iida, H., Tsukagoshi, S., and Sakurai, Y. (1981). Overcoming of vincristine resistance in p388 leukemia in vivo and in vitro through enhanced cyto-toxicity of vincristine and vinblastine by verapamil. Cancer Research *41*, 1967-1972.

Tu, Y., Gardner, A. and Lichtenstein, A., (2000). The phosphatidylinositol 3-kinase/AKT kinase pathway in multiple myeloma plasma cells: roles in cytokine-dependent survival and proliferative responses. Cancer Research *60*, 6763-6700.

Turchinovich, A., Weiz, L., Langheinz, A., and Burwinkel, B. (2011). Characterization of extracellular circulating microRNA. Nucleic Acids Research *39*, 7223-7233.

Turner, J.G., Gump, J.L., Zhang, C., Cook, J.M., Marchion, D., Hazlehurst, L., Munster, P. et al. (2006). ABCG2 expression, function, and promoter methylation in human multiple myeloma. Blood *108*, 3881-3889.

Van Deun, J., Mestdagh, P., Sormunen, R., Cocquyt, V., Vermaelen, K., Vandesompele, J., Bracke, M., De Wever, O., and Hendrix, A. (2014). The impact of disparate isolation methods for extracellular vesicles on downstream RNA profiling. J Extracell Vesicles *3*.

Voorhees, P. M., Chen, Q., Kuhn, D.J., Small, G.W., Hunsucker, S.A. and Strader, J.S. (2007). Inhibition of interleukin-6 signaling with CNTO 328 enhances the activity of bortezomib in preclinical models of multiple myeloma. Clin Cancer Res *13(21)*, 6469-6478.

Walker, B.A., Wardell, C.P., Brioli, A., Boyle, E., Kaiser, M.F., Begum, D.B., Dahir, N.B. et al. (2014). Translocations at 8q24 juxtapose MYC with genes that harbor superenhancers resulting in overexpression and poor prognosis in myeloma patients. Blood Cancer Journal *4*, e191.

Wang, X., Li, C., Ju, S., Wang, Y., Wang, H., and Zhong, R. (2011). Myeloma cell adhesion to bone marrow stromal cells confers drug resistance by microRNA-21 up-regulation. Leukemia & Lymphoma *52*, 1991-1998.

Wang, J., Hendrix, A., Hernot, S., Lemaire, M., De Bruyne, E., Van Valckenborgh, E., Lahoutte, T., De Wever, O., Vanderkerken, K., and Menu, E. (2014). Bone marrow stromal cell-derived exosomes as communicators in drug resistance in multiple myeloma cells. Blood 124, 555-566.

Wuillème-Toumi, S., Robillard, N., Gomez, P., Moreau, P., Le Gouill, S., Avet-Loiseau, H., Harousseau, J.L., Amiot, M. and Bataille, R. (2005). Mcl-1 is overexpressed in multiple myeloma and associated with relapse and shorter survival. Leukemia *19(7),*1248-52.

Yanez-Mo, M., Siljander, P.R.M., Andreu, Z., Zavec, A.B., Borras, F.E., Buzas, E.I., Buzas, K., Casal, E., Cappello, F., Carvalho, J., et al. (2015). Biological properties of extracellular vesicles and their physiological functions. Journal of extracellular vesicles 4, 27066-27066.

Yang, H.H., Ma, M.H., Vescio, R.A., and Berenson, J.R. (2003). Overcoming drug resistance in multiple myeloma: the emergence of therapeutic approaches to induce apoptosis. Journal of clinical oncology : official journal of the American Society of Clinical Oncology *21*, 4239-4247.

Yang, W.-C.L., Sheng-Fung Mechanisms of Drug Resistance in Relapse and Refractory Multiple Myeloma. BioMed Research International.

Yoshioka, Y., Konishi, Y., Kosaka, N., Katsuda, T., Kato, T., and Ochiya, T. (2013). Comparative marker analysis of extracellular vesicles in different human cancer types. J Extracell Vesicles *2*.

Zhang, X., Yuan, X., Shi, H., Wu, L., Qian, H. and Xu, W. (2015). Exosomes in cancer: small particle, big player. Journal of Hematology & Oncology *8:83*.

Zhang, L., Fok, J.H.L. and Davies, F.E. (2014). Heat shock proteins in multiple myeloma. Oncotarget *5*, 1132-1148.

Zhao, L., Liu, W., Xiao, J. and Cao, B. (2015). The role of exosomes and "exosomal shuttle microRNA" in tumorigenesis and drug resistance. Cancer Letters *356*, 339–346.

Zhu, Y.X., Braggio, E., Shi, C.X., Bruins, L.A., Schmidt, J.E., Van Wier, S., Chang, X.B., Bjorklund, C.C., Fonseca, R., Bergsagel, P.L., et al. (2011). Cereblon expression is required for the antimyeloma activity of lenalidomide and pomalidomide. Blood *118*, 4771-4779.

Zhu, Y.X., Braggio, E., Shi, C.X., Kortuem, K.M., Bruins, L.A., Schmidt, J.E., Chang, X.B., Langlais, P., Luo, M., Jedlowski, P., et al. (2014). Identification of cereblon-binding proteins and relationship with response and survival after IMiDs in multiple myeloma. Blood *124*, 536-545.